Role of transverse effects in laser instabilities

L. A. Lugiato
Dipartimento di Fisica, Politecnico di Torino, Torino, Italy

F. Prati
Dipartimento di Fisica, Università di Milano, Milano, Italy

L. M. Narducci, P. Ru, and J. R. Tredicce
Physics Department, Drexel University, Philadelphia, Pennsylvania 19104

D. K. Bandy
Physics Department, Oklahoma State University, Stillwater, Oklahoma 74078
(Received 10 August 1987)

We generalize the traditional Maxwell-Bloch theory of a ring laser and analyze the dynamical role of transverse effects. With the help of a suitable extension of the uniform-field limit we perform an essentially analytical study of the steady-state and linear-stability properties of a ring resonator containing a homogeneously broadened active medium. In this context we incorporate the effects of curved reflecting surfaces, the possible lack of transverse uniformity of the pump, and the detailed structure of the cavity modes. In the uniform-field limit we prove that the laser steady state is of the single-mode variety and that lack of stability can be induced in this field configuration even only a few percent above the threshold for laser action. Thus our main claim is that transverse effects can be responsible for low threshold instabilities. This explanation is more plausible to explain the observed pulsations in many lasers than what is available in terms of the traditional plane-wave theories.

I. INTRODUCTION

One of the unexpected features of early laser systems was the appearance of output pulsations even under steady or nearly steady pumping conditions. In fact, spiking had already been observed in maser experiments[1] even before the discovery of the laser; with the proliferation of solid-state optical devices, this effect acquired the status of a nearly universal feature.[2] The interpretation of these phenomena as direct manifestations of intrinsic dynamic instabilities, linked to the nonlinear character of the emission, should be ranked among the most significant theoretical advances of the late 1950s and early 1960s.[3,4]

The most common modern framework for the description of laser dynamics is the plane-wave Maxwell-Bloch model, a formulation flexible enough to conform to most experimental conditions and capable of yielding a detailed insight into the laser working mechanism. Yet for all the important contributions that this model has made to laser physics, it has also shown a consistent pattern of quantitative disagreement, and even qualitative disagreement, with experimental facts, especially when the instabilities become a dominant dynamical feature.[5]

An important starting point for our discussion is the recognition that the plane-wave Maxwell-Bloch equations do predict the existence of instabilities leading to both regular and chaotic pulsations; this is a well-established theoretical fact.[6] Thus homogeneously broadened systems are known to produce output oscillations when operating both in single-mode and multimode configurations, and in and out of resonance, relative to the center of the atomic gain line. Of special significance is the existence of an isomorphism between the single-mode laser model and the Lorenz equations.[6(a)] The Lorenz equations, originally derived to simulate the onset of convective instabilities,[7] are well known in the mathematical literature as the paradigm of deterministic chaos.[8] Thus the isomorphism between the laser and the Lorenz equations supports the notion that the laser itself can be the source of chaotic behavior.

While the link between the observed laser pulsations and dynamic instabilities is a very reasonable theoretical proposition, the prediction that these phenomena can occur only for very large values of the pump parameter, especially under resonant conditions, is the source of major difficulties with the interpretation of experimental results. Indeed, if one took the theoretical threshold values too seriously, one would have to conclude that laser instabilities are observable only under exceptional circumstances.

An additional difficulty with the plane-wave Maxwell-Bloch equations is the unconditional stability of their rate-equation limit. Accepting this result leads to the conclusion that all laser instabilities are manifestations of atomic coherence, this assertion is hardly in agreement with the behavior of ruby, Nd:yttrium aluminum garnet, CO_2, and other lasers for which the validity of the rate-equation description is well justified.

Better agreement between theory and experiments is obtained when the laser undergoes a phase instability,[6(g)] a phenomenon that requires operation under detuned

conditions and which is responsible, for example, for the observed mode hopping in CO_2 laser systems.[9] However, the physical mechanism that drives a phase instability is quite different from that which is operative under resonant conditions (i.e., the amplitude instability[10]), so that the theory of phase instabilities is not very helpful in clarifying the nature of the "high second threshold problem." The theory of inhomogeneously broadened lasers is also in good qualitative agreement with the observed unstable phenomena;[11] in this case, the lowering of the second laser threshold to the observed experimental range[12] is probably due to the large increase in the number of degrees of freedom that are needed to describe the laser dynamics, and offers little information for the failing of the homogeneously broadened model.

It is probably fair to say that the plane-wave approximation, long viewed as adequate in capturing the essential aspects of laser dynamics, may be a much stronger theoretical constraint than anticipated. In fact, important warning signals in this direction came from the lack of quantitative agreement between the predictions of the plane-wave studies of optical bistability[13] and the careful absolute measurements performed by Kimble and collaborators under steady-state conditions.[14] If, however, these theoretical propositions were in disagreement with the experiments in a quantitative way, more serious qualitative discrepancies have emerged from the study of self-pulsing in bistable systems. Here the plane-wave theory predicts a rich variety of dynamical behaviors[15] which do not appear to have a counterpart among the observed patterns.[16]

The main objective of this paper is to produce evidence that transverse degrees of freedom play a far more important role in laser dynamics than might be expected. In fact, we have known for some time that transverse effects can have a strong influence on the stationary and dynamic behavior of passive driven systems,[17] and that plane-wave and transverse models can approach chaos by way of very different routes.[18] The combined message of a small but growing number of experimental[19] and theoretical reports[20] supports the belief that effects related to a departure from the plane-wave configuration may be even more influential when the optical resonator contains an active rather than a passive medium. If we accept this premise, the inclusion of transverse degrees of freedom into the existing theories becomes a necessary requirement for a successful description of realistic laser systems.

Indeed, several theoretical studies have already attempted to improve on the plane-wave description. An analysis of the modes and of their spatial stability in a realistic resonator can be found, for example, in Ref. 21. Reference 22 contains a study of the emission frequency of an inhomogeneously broadened laser when the field configuration is no longer of the pure Gaussian type. The problem of laser dynamics in the presence of transverse effects was addressed in Ref. 23, using an approximate set of equations, and evidence was presented for the appearance of self-pulsing.

A useful alternative approach is based on the assumption that the cavity field maintains a fixed Gaussian profile during the evolution.[17(b),24] On the surface this appears to be a rather crude approximation because the presence of an active medium may be expected to introduce significant distortion in the transverse pattern of the field. In the case of passive systems, however, this approach has yielded quite reasonable results,[25] perhaps because of the constraints that the injected mode-matched signal imposes on the cavity field. The situation is likely to be more critical with active systems, so a more realistic approach may be required. In fact, even the simple Gaussian model of the laser yields remarkable deviations from the plane-wave behavior; the Risken and Nummedal instability[6(b),6(c)] of the longitudinal sidebands, for example, is suppressed under resonant conditions if the cavity field has a TEM_{00} profile.[24]

In this study we consider those physical and geometrical features that are absent by definition from the plane-wave theory. To be specific, we focus on the effects of diffraction, on the wave-front curvature induced by the spherical mirrors, and on the transverse and longitudinal gain variations caused by the pump mechanism. It would also be very desirable to consider the effects of limiting intracavity apertures, but this aspect of the problem is more complicated and will be omitted from this study.

Of course the mathematical description of this problem is considerably more involved than in the case of a plane-wave model, and significant theoretical progress is likely to require large-scale numerical calculations when the parameters of the system take on arbitrary values. An unavoidable drawback of most numerical approaches is that a global understanding usually requires the analysis of a wide region of the parameter space. For this reason it is much more desirable to investigate transverse effects by analytical means, as much as feasible. Of course this cannot be done for arbitrary configurations of the laser system. Fortunately it is possible to identify a nontrivial setting that allows significant theoretical progress with a minimum of numerical labor. Our approach is based on an appropriate extension of the well-known uniform-field limit,[26] a model that has played a major role in defining our current understanding of the plane-wave theories of active and passive systems. In spite of its idealized nature, the uniform-field limit of the plane-wave model has led to predictions that are in remarkably close qualitative agreement with the results of the exact linear-stability analysis[27] and with the numerical solutions of the Maxwell-Bloch equations.[28] It is hoped that the same conclusion will remain valid in the presence of transverse effects. Much more work, however, will be needed to confirm this conjecture.

An important consequence of this limit, as we show in this paper, is that the steady-state solutions are of the single-mode type, a conclusion which also implies that the empty cavity modes are also exact modes of the filled cavity in the uniform-field limit. This statement is true in the plane-wave approximation and remains valid in the presence of transverse effects. Thus, at once, the mathematical description of the problem is simplified to a large extent, and earlier studies based on the single transverse mode approximation[17(e),24] can be understood in rigorous terms.

With the assumption that the cavity linewidth is much smaller than the atomic decay rates, the so-called "good cavity" limit, we can describe the emergence of unstable states through a development that rests almost entirely on analytic grounds; in fact, only the final evaluation of the rates of evolution of the fluctuation variables requires a numerical computation. The linear-stability analysis leads to one of the most interesting results: The instability thresholds for a fairly realistic cavity design are much closer to the first laser threshold than predicted by the plane-wave theory, and are in much better quantitative agreement with the experimental picture. For example, under appropriate conditions, unstable operation emerges when the pump parameter is only a few percent above threshold, while the plane-wave theory requires pump-parameter values at least ten times larger than needed to produce laser emission.

We show, in addition, that low threshold instabilities can be found also in the full adiabatic elimination limit, i.e., when the dynamics of the laser is described entirely by the field equation (thus *a fortiori* the same conclusion holds in the rate-equation limit when only the polarization is eliminated adiabatically). According to this result instabilities are not necessarily a consequence of atomic coherence, in contrast with the predictions of the plane-wave theory.

The physical setting of the linear-stability analysis is the following: With the laser operating in steady state, we look for the existence of unstable modes, as evidenced by the appearance of an exponential growth for the field fluctuations. This approach to the problem is conceptually identical to the one adopted by Risken and Nummedal[6(b),6(c)] in their classic study of multimode instabilities, although there are also significant differences, as we shall discuss in Secs. III and IV.

In Sec. II we construct the empty cavity eigenfunctions and eigenfrequencies for a folded-ring resonator. In Sec. III we describe the extended Maxwell-Bloch model, we introduce the uniform-field limit, and we calculate the steady-state configuration of the system, which we then analyze for different values of the parameters. In Sec. IV we outline the details of the linear-stability analysis. In Sec. V we discuss the results of this calculation, give evidence for the existence of low threshold instabilities, and show how these effects persist even after adiabatic elimination of all the atomic variables. We conclude, in Sec. VI, with a brief overview and some general comments. A preliminary account of this work can be found in Ref. 29.

II. THE EMPTY CAVITY MODES

This section contains a brief description of a calculation leading to the modal eigenfunctions and eigenfrequencies of an empty resonator in the paraxial approximation.[30] Its purpose is to provide a self-contained introduction to the basic tools that will be used extensively in our subsequent calculations. The reader who is already familiar with this type of calculation can proceed directly to Sec. III for a discussion of the main problem.

The analysis of an empty resonator of length Λ, as shown in Fig. 1, begins with the free-field wave equation

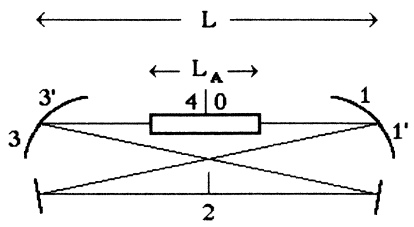

FIG. 1. Schematic representation of the ring cavity. The entire length of the folded resonator is Λ; the length of the active medium is L_A and the separation between the spherical mirrors is L. Point 0 marks the origin of the reference system that measures the position along the axis of the cavity, while point 4 denotes the end of a full loop. Points 1 and 1', 3 and 3' denote the longitudinal positions just before and after reflection, respectively. Point 2 is located at half a round trip.

$$\nabla_2 E(r,z,t)-\frac{1}{c^2}\frac{\partial^2}{\partial t^2}E(r,z,t)=0\ , \tag{2.1}$$

where z is the coordinate along the axial direction of propagation of the field and r is the radial coordinate measured from the axis of symmetry of the system. As implied by Eq. (2.1), we consider a system with cylindrical symmetry.

In the paraxial approximation we seek elementary solutions of the form

$$E\equiv E_p(r,z,t)=A_p(r,z)e^{i(k_p z-\omega_p t)}\ . \tag{2.2}$$

In fact, the solutions corresponding to a cylindrically symmetric system should be labeled by two indices related to the axial and radial degrees of freedom, respectively. We will omit the axial modal index, for simplicity, except where necessary.

In the slowly-varying-amplitude approximation, and in terms of the scaled coordinates

$$\eta=z/L,\quad \rho=\left[\frac{\pi}{L\lambda_p}\right]^{1/2} r\ , \tag{2.3}$$

where L is the distance between the curved mirrors, the wave equation takes the form

$$\frac{\partial A_p}{\partial \eta}=\frac{i}{4}\left[\frac{\partial^2}{\partial\rho^2}+\frac{1}{\rho}\frac{\partial}{\partial\rho}\right]A_p\ , \tag{2.4}$$

whose solutions are

$$A_p(\rho,\eta)=\frac{2}{v(\eta)}L_p\left[\frac{2\rho^2}{v^2(\eta)}\right]\exp\left[-\frac{\rho^2}{v^2(\eta)}\right]\times\exp\left[i\left[\frac{\rho^2}{u(\eta)}-(2p+1)\tan^{-1}\eta/\eta_0\right]\right]\ ,$$
$$p=0,1,2,\ldots\ . \tag{2.5}$$

The origin of the longitudinal axis is selected at point 0 of Fig. 1, where $E_p(\rho,\eta,t)$ has a plane-wave structure. The functions $v(\eta)$ and $u(\eta)$ are defined by

$$v(\eta)=\sqrt{\eta_0}[1+(\eta/\eta_0)^2]^{1/2}\ , \tag{2.6a}$$

$$u(\eta)=\frac{1}{\eta}(\eta^2+\eta_0^2)\ , \tag{2.6b}$$

and $\eta_0=v^2(0)\equiv v_0^2$ is an arbitrary parameter which must be calculated to conform with the cavity geometry. Note that with the selected scaling (2.3), η_0 is the Rayleigh range of the Gauss-Laguerre beam (2.5), while $\sqrt{\eta_0}$ is the beam waist.

The assignment of η_0 stems from the following considerations. The beam parameter $q(\eta)$ defined by

$$\frac{1}{q(\eta)}=\frac{1}{u(\eta)}+\frac{i}{v^2(\eta)} \tag{2.7}$$

satisfies elementary mapping rules under translations and reflections from the curved surfaces. Beginning with a given beam parameter q_0 at position 0, we can easily construct the beam parameter q_4 after one full loop (Fig. 1). The condition $q_4=q_0$ secures that the beam parameter after one round trip acquires the same starting value.

For simplicity we select a cavity with a high degree of longitudinal symmetry, as shown in Fig. 1. This leads to[30]

$$\eta_0=v_0^2=\frac{1}{2}\left[\frac{(\rho_0-1)(\rho_0-1+f)}{f(1+\rho_0)-1}\right]^{1/2}\ , \tag{2.8}$$

where $\rho_0=R/L$ is the scaled radius of curvature of the spherical mirrors and the parameter f is defined by L/Λ.

In a similar way we can construct the analytic form of the modal functions $A_p(\rho,\eta)$ for $\frac{1}{2}\le\eta\le\Lambda/L-\frac{1}{2}$. The beam waist in this case is given by

$$v_2^2=\frac{1}{\mathrm{Im}\left[\dfrac{1}{q_2}\right]}\ ,$$

where q_2 is the beam parameter at $\eta=\Lambda/2L$ (point 2 of Fig. 1). The explicit form of the modal functions in this range is

$$A_p(\rho,\eta)=B_p[q_2(\eta-\Lambda/2L)]\times\exp\left[-i(2p+1)\tan^{-1}\left[\frac{\eta-\Lambda/2L}{v_2^2}\right]\right]e^{i\varphi}\ , \tag{2.9}$$

where, for convenience, we have defined

$$B_p[q_2(\eta)]=\frac{2}{v_2(\eta)}L_p\left[\frac{2\rho^2}{v_2^2(\eta)}\right]\times\exp\left[-\frac{\rho^2}{v_2^2(\eta)}+i\frac{\rho^2}{u_2(\eta)}\right]\ . \tag{2.10}$$

The functions $v_2(\eta)$ and $u_2(\eta)$ are defined by Eqs. (2.6), with η_0 replaced by

$$v_2^2=v^2(\Lambda/2L)=\frac{1}{\rho_0^2\eta_0}\left[\eta_0^2\left[\frac{1}{f}-1-\rho_0\right]^2+\frac{1}{4}\left[\frac{\rho_0-1}{f}+1\right]^2\right]\ . \tag{2.11}$$

The phase factor $e^{i\varphi}$ measures the shift introduced by the free propagation along the segment $1'\to2$ in Fig. 1. This phase factor can be calculated by matching Eq. (2.9) at position 1' (i.e., $\eta=\frac{1}{2}$) with the field given by Eq. (2.5) after a reflection from the first spherical mirror. The reflection for near normal incidence is simulated by the operator

$$\mathcal{R}=\exp\left[-i\frac{2\rho^2}{\rho_0}\right]\ . \tag{2.12}$$

It follows at once that

$$\varphi=-(2p+1)\left[\tan^{-1}\left[\frac{1}{2v_0^2}\right]+\tan^{-1}\left[\frac{1/f-1}{2v_2^2}\right]\right]\ . \tag{2.13}$$

In addition, after a full loop, the empty cavity solution A_p at position 4 is related to the solution at position 0 by the equation

$$A_p(4)=e^{2i\varphi}A_p(0)\ . \tag{2.14}$$

Now we calculate the empty cavity resonances. The boundary condition for the elementary radial solution of order p is

$$E_p(\rho,0,t)=E_p(\rho,\Lambda/L,t)\ , \tag{2.15}$$

or

$$A_p(0)=e^{i\omega_p\Lambda/c}A_p(4) \tag{2.16}$$

when expressed in terms of the modal amplitudes A_p. From Eqs. (2.16), (2.14), and (2.13) we have

$$\omega_{n,p}\frac{\Lambda}{c}=2\pi n+2(2p+1)\times\left[\tan^{-1}\left[\frac{1}{2v_0^2}\right]+\tan^{-1}\left[\frac{1/f-1}{2v_2^2}\right]\right]\ , \tag{2.17}$$

with $n=0,\pm1,\pm2,\ldots$ and $p=0,1,2,\ldots$. The eigenfrequencies are labeled by two indices, an axial index n and a transverse index p. The longitudinal intermode spacing is given by the usual formula $2\pi nc/\Lambda$, while the frequency separation between adjacent transverse modes is

$$(\omega_{n,p+1}-\omega_{n,p})\equiv\delta\omega_1=4\frac{c}{\Lambda}\left[\tan^{-1}\left[\frac{1}{2v_0^2}\right]+\tan^{-1}\left[\frac{1/f-1}{2v_2^2}\right]\right]\ . \tag{2.18}$$

An important property of the modal functions $A_p(\rho,\eta)$ is that for every value of η they form an orthonormal set in the sense that

$$\int_0^\infty d\rho\,\rho\,A_p^*(\rho,\eta)A_{p'}(\rho,\eta)=\delta_{p,p'}\ . \tag{2.19}$$

With the additional reasonable assumption that

$\{A_p(\rho,\eta)\}$ form a complete set with respect to the radial coordinate, these functions provide a useful basis for the expansion of any cavity field at every point along the η axis. This property will play an essential role in the following development.

III. THE GENERALIZED MAXWELL-BLOCH PROBLEM: DESCRIPTION OF THE MODEL AND THE STEADY-STATE SOLUTION

A. Derivation of the equations

We extend the traditional description of the laser with the inclusion of several features that are omitted, by definition, from the plane-wave theory.

(i) The diffraction caused by the finite transverse cross section of the field and by its radial variations of amplitude and phase.

(ii) The wave-front curvature imposed by the presence of reflecting spherical surfaces.

(iii) The longitudinal and radial variations of the equilibrium population difference.

We do so in the context of the paraxial approximation and under the assumption of cylindrical symmetry for the field and for the atomic variables. The latter restriction, in particular, is a compromise dictated by the need for including transverse degrees of freedom with the lowest level of analytic and numerical complexity. We recognize that this is not a very realistic setting for a typical laser but, nevertheless, we expect that it will provide useful insights into the role of transverse effects.

One can model the effects of diffraction by adding a term of the form $\nabla_\perp F$ to the usual wave equation for the slowly varying amplitude F where

$$\nabla_\perp = \frac{\partial^2}{\partial r^2} + \frac{1}{r}\frac{\partial}{\partial r} \tag{3.1}$$

is the transverse Laplacian for an axially symmetric geometry. The curved reflectors affect the boundary conditions indirectly by way of the dependence of the radial eigenfrequencies on the radius of curvature of the mirrors [see Eq. (2.17)], as we shall discuss more explicitly below. Finally, the longitudinal and transverse variations of the pump are reflected in the equilibrium value of the population difference, which is no longer uniform along the transverse direction as in the plane-wave model.

With these modifications the Maxwell-Bloch equations take the form

$$\frac{\partial F}{\partial \eta} + \frac{1}{v}\frac{\partial F}{\partial \tau} = \frac{i}{4}\left[\frac{\partial^2 F}{\partial \rho^2} + \frac{1}{\rho}\frac{\partial F}{\partial \rho}\right] - \alpha L P \ , \tag{3.2a}$$

$$\frac{\partial P}{\partial \tau} = -[FD + (1 + i\delta'_{AC})P] \ , \tag{3.2b}$$

$$\frac{\partial D}{\partial \tau} = -\gamma[-\tfrac{1}{2}(F^*P + FP^*) + D - \chi(\rho,\eta)] \ . \tag{3.2c}$$

We select as the cavity reference frequency ω_0 the $p=0$ empty cavity resonance $\omega_{n,0}$, so that the slowly varying field amplitude F is related to the Maxwell field by

$$E(r,z,t) = \frac{\hbar\sqrt{\gamma_\perp \gamma_\parallel}}{2\mu}\tfrac{1}{2}[F(r,z,t)e^{i(k_0 z - \omega_0 t)} + \text{c.c.}] \ , \tag{3.3}$$

where μ is the modulus of the atomic transition dipole moment and $\gamma_\perp$ and $\gamma_\parallel$ are the polarization and population decay rates, respectively, and $k_0 = \omega_0/c$. The spatial coordinates η and ρ are defined by Eqs. (2.3) with λ_p replaced by λ_0 (the reference wavelength); τ, v, and δ'_{AC} are defined by

$$\tau = \gamma_\perp t, \quad v = \frac{c}{L\gamma_\perp}, \quad \delta'_{AC} = \frac{\omega_A - \omega_0}{\gamma_\perp} \ , \tag{3.4}$$

where ω_A is the atomic transition frequency; the parameter γ denotes the ratio $\gamma_\parallel/\gamma_\perp$ and the function $\chi(\rho,\eta)$ simulates the longitudinal and transverse variations of the pump. There is a good deal of flexibility in the choice of χ, depending on the details of the excitation system. For definiteness we select

$$\chi(\rho,\eta) = \begin{cases} \chi'(\rho) & \text{for } |\eta| < \dfrac{L_A}{2L} \\ 0 & \text{otherwise} \ , \end{cases} \tag{3.5a}$$

where L_A denotes the length of the medium, and consider, as two possible models, the radial functions

$$\chi'(\rho) = \exp\left[-\frac{\rho^2}{2\rho_P^2}\right] \tag{3.5b}$$

and

$$\chi'(\rho) = 2\exp\left[-\frac{\rho^2}{2\rho_P^2}\right] - 1 \ . \tag{3.5c}$$

In the first case the active medium is transparent at the outer boundaries of the pumped volume (this model is plausible, for example, in the case of a four-level system such as Nd:YAG), while in the second case lowering the pump strength creates an absorbing region, such as one may find in a ruby laser, for example.

A way to state the boundary conditions is to require that the Maxwell field at position $\eta=0$ matches the field that has reached the position $\eta=\Lambda/L$ after propagating one full loop through the cavity. Formally this implies

$$E(\rho,0,\tau) = E(\rho,\Lambda/L,\tau) \ , \tag{3.6a}$$

or, in terms of the slowly varying amplitude,

$$F(\rho,0,\tau) = F(\rho,\Lambda/L,\tau)e^{i\omega_0\Lambda/c} \ . \tag{3.6b}$$

Equation (3.6b) must be understood as the assignment that sets the slowly varying field amplitude at the boundary $\eta=0$ and at time τ in terms of the amplitude that has just completed one loop through the cavity according to Eqs. (3.2), and in compliance with the appropriate reflections at the curved surfaces. This type of boundary condition is especially appropriate in connection with the numerical solution of Eqs. (3.2). In the following we carry out our analysis of the steady state and of the linear stability in terms of a modal expansion of the field so that a different version of the boundary conditions is required.

As our starting point we let

$$F(\rho,\eta,\tau)=e^{-i\delta\Omega'\tau}\mathbf{F}(\rho,\eta,\tau)$$
$$=e^{-i\delta\Omega'\tau}\sum_p A_p(\rho,\eta)f_p(\eta,\tau)\ , \tag{3.7a}$$

$$P(\rho,\eta,\tau)=e^{-i\delta\Omega'\tau}\mathbf{P}(\rho,\eta,\tau)\ , \tag{3.7b}$$

where $\delta\Omega'$ is the offset between the unknown operating laser frequency and the reference frequency ω_0 in units of $\gamma_\perp$. We substitute Eqs. (3.7) into the Maxwell-Bloch equations (3.2) and integrate over the radial variable with the help of the orthogonality integral (2.19). The result is the following set of coupled equations for the modal amplitudes $f_p(\eta,\tau)$ and for the atomic variables:[17(e)]

$$\frac{\partial f_p}{\partial\eta}+\frac{1}{v}\frac{\partial f_p}{\partial\tau}=i\frac{\delta\Omega'}{v}f_p-\alpha L\int_0^\infty d\rho\,\rho\,A_p^*(\rho,\eta)\mathbf{P}(\rho,\eta,\tau)\ , \tag{3.8a}$$

$$\frac{\partial\mathbf{P}}{\partial\tau}=-[\mathbf{F}D+(1+i\Delta')\mathbf{P}]\ , \tag{3.8b}$$

$$\frac{\partial D}{\partial\tau}=-\gamma[-\tfrac{1}{2}(\mathbf{F}^*\mathbf{P}+\mathbf{F}\mathbf{P}^*)+D-\chi(\rho,\eta)]\ , \tag{3.8c}$$

where $\Delta'=\delta'_{AC}-\delta\Omega'$. The modal amplitudes obey the boundary conditions

$$f_p(-1/2,\tau)=Re^{-i\delta_p}\exp\left[i\delta\Omega'\gamma_\perp\frac{\Lambda-L}{c}\right]$$
$$\times f_p\left[\frac{1}{2},\tau-\gamma_\perp\frac{\Lambda-L}{c}\right]\ , \tag{3.8d}$$

where $\delta_p\equiv(\omega_{n,p}-\omega_0)\Lambda/c$ and R denotes the reflectivity of the mirrors; a brief outline of the derivation of Eq. (3.8d) is given in Appendix A. Note that the sum in Eq. (3.7a) extends to all non-negative integers p. In practice, however, transverse modes with p greater than 1 or 2 suffer significant diffraction losses, typically because of intracavity apertures. We do not have provisions in our treatment for describing this type of losses; we must keep in mind, however, that only very few transverse modes are expected to play a significant dynamical role in the evolution of a real laser.

In steady state the atomic variables are given by

$$\mathbf{P}_{\rm st}=-\chi\mathbf{F}_{\rm st}\frac{1-i\Delta'}{1+\Delta'^2+|\mathbf{F}_{\rm st}|^2}\ , \tag{3.9a}$$

$$D_{\rm st}=\chi\frac{1+\Delta'^2}{1+\Delta'^2+|\mathbf{F}_{\rm st}|^2}\ , \tag{3.9b}$$

and the equation for the modal amplitudes becomes

$$\frac{\partial f_p}{\partial\eta}=i\frac{\delta\Omega'}{v}f_p$$
$$+\alpha L(1-i\Delta')$$
$$\times\int_0^\infty d\rho\,\rho\,A_p^*(\rho,\eta)\chi(\rho,\eta)\frac{\mathbf{F}_{\rm st}}{1+\Delta'^2+|\mathbf{F}_{\rm st}|^2}\ , \tag{3.10}$$

where

$$\mathbf{F}_{\rm st}(\rho,\eta)=\sum_p A_p(\rho,\eta)f_p(\eta)\ . \tag{3.11}$$

Even the steady-state problem, in general, offers formidable analytic difficulties. Important simplifications follow in the limit

$$\alpha L_A\to 0,\quad T\to 0\quad\left[2C=\frac{\alpha L_A}{T}\text{ is arbitrary}\right], \tag{3.12a}$$

and

$$|\delta_p-2\pi m|=O(1) \tag{3.12b}$$

for all $p\neq 0$ and $m=0,\pm1,\pm2,\ldots$. The symbol $T=1-R$ denotes the mirror transmittivity. Equation (3.12a) is well known from earlier studies of optical instabilities in the plane-wave regime.[26] Equation (3.12b) implies that the frequency separation between adjacent radial modes should be of the same order of magnitude as the frequency spacing between longitudinal resonances, and simultaneously excludes degeneracies or quasidegeneracies between transverse and longitudinal modes. The two conditions (3.12) taken together define the extended uniform-field limit for the chosen laser system. Of course, it is understood that the label "uniform-field limit" should not be taken literally. What is actually independent of η, in this limit, is the set of modal amplitudes $\{f_p\}$. The field profile inside the cavity is assigned by the modal functions $\{A_p\}$, which, of course, depend on the longitudinal coordinate η.

The importance of the uniform-field limit in this context rests on its ability to provide a strong analytic contribution to the solution of the laser equations of motion and a deeper view into the role that the many parameters play in setting the stationary and dynamical properties of the system. As we shall prove below, the stationary state of the laser field in the uniform-field limit is of the single longitudinal and transverse mode type; as a consequence, it follows that the empty cavity eigenfunctions, in this limit, are also modes of the resonator in the presence of the active medium.

We now return our attention to the solution of the stationary modal equations (3.10) under the conditions (3.12). The spatial integral of Eq. (3.10) yields

$$f_p(1/2)-f_p(-1/2)=i\frac{\delta\Omega'}{v}\int_{-1/2}^{1/2}d\eta\,f_p+\alpha L(1-i\Delta')\int_{-1/2}^{1/2}d\eta\int_0^\infty d\rho\,\rho\,A_p^*\chi\frac{\mathbf{F}_{\rm st}}{1+\Delta'^2+|\mathbf{F}_{\rm st}|^2}\ . \tag{3.13}$$

Assuming that $\delta\Omega'\gamma_\perp\Lambda/c$ is of the order of T, the boundary conditions (3.8) in steady state can also be cast into the approximate forms

$$f_0(1/2)-f_0(-1/2)=T\left[1-i\frac{\delta\Omega'}{T}\gamma_\perp\frac{\Lambda-L}{c}\right]f_0(1/2)\quad(p=0)\,, \tag{3.14a}$$

$$f_p(1/2)-f_p(-1/2)=\left[1-Re^{-i\delta_p}\exp\left[i\delta\Omega'\gamma_\perp\frac{\Lambda-L}{c}\right]\right]f_p(1/2)\quad(p\neq 0)\,. \tag{3.14b}$$

If we combine Eqs. (3.14) with Eq. (3.12) we obtain

$$\begin{aligned}f_0(1/2)-f_0(-1/2)&=T\left[1-i\frac{\delta\Omega'}{T}\gamma_\perp\frac{\Lambda-L}{c}\right]f_0(1/2)\\&=i\frac{\delta\Omega'}{v}\int_{-1/2}^{1/2}d\eta f_0+\alpha L(1-i\Delta')\int_{-1/2}^{1/2}d\eta\int_0^\infty d\rho\rho A_0^*\chi\frac{\mathbf{F}_{\rm st}}{1+\Delta'^2+|\mathbf{F}_{\rm st}|^2}\quad(p=0)\,,\end{aligned} \tag{3.15a}$$

$$\begin{aligned}f_p(1/2)-f_0(-1/2)&=\left[1-Re^{-i\delta_p}\exp\left[i\delta\Omega'\gamma_\perp\frac{\Lambda-L}{c}\right]\right]f_p(1/2)\\&=i\frac{\delta\Omega'}{v}\int_{-1/2}^{1/2}d\eta f_p+\alpha L(1-i\Delta')\int_{-1/2}^{1/2}d\eta\int_0^\infty d\rho\rho A_p^*\chi\frac{\mathbf{F}_{\rm st}}{1+\Delta'^2+|\mathbf{F}_{\rm st}|^2}\quad(p\neq 0)\,.\end{aligned} \tag{3.15b}$$

Equations (3.15) lead to the following conclusions.

(i) The difference $f_0(1/2)-f_0(-1/2)$ is of the order of T, so that f_0 is uniform along the axial direction; in fact, in view of Eq. (3.5a), L can be replaced by L_A in Eqs. (3.15) and, by assumption, αL_A and T are of the same order of magnitude [see Eq. (3.12a)].

(ii) The amplitudes f_p with $p\neq 0$ is of the order of T.

Hence it follows that in the uniform-field limit a possible steady-state solution is characterized by the modal amplitudes $f_0=O(1)$, $f_{p\neq 0}=O(T)$ and the cavity field configuration is of the TEM_{00} type.

The immediate consequence of these considerations is the state equation

$$1-i\frac{\delta\Omega'}{T}\gamma_\perp\frac{\Lambda}{c}=2C(1-i\Delta')\frac{L}{L_A}\int_{-L_A/2L}^{+L_A/2L}d\eta\int_0^\infty d\rho\rho\chi'\frac{|A_0(\rho,\eta)|^2}{1+\Delta'^2+|A_0(\rho,\eta)f_0|^2} \tag{3.16}$$

for the modal amplitude f_0, where we have taken Eq. (3.5a) into account. This can be split into real and imaginary parts with the result

$$1=2C\frac{L}{L_A}\int_{-L_A/2L}^{+L_A/2L}d\eta\times\int_0^\infty d\rho\rho\chi'\frac{|A_0(\rho,\eta)|^2}{1+\Delta'^2+|A_0(\rho,\eta)f_0|^2}\,, \tag{3.17a}$$

$$\delta\Omega'=\kappa'\Delta'\ \text{ or }\ \delta\Omega'=\frac{\kappa'}{1+\kappa'}\delta'_{AC}\,, \tag{3.17b}$$

where $\kappa'=cT/\Lambda\gamma_\perp$ denotes the cavity linewidth in units of $\gamma_\perp$. Equation (3.17b) is a disguised form of the usual mode-pulling formula, which remains unchanged in the uniform-field limit even in the presence of transverse effects.

The stationary state (3.17) is not unique because, depending on the gain parameter $2C$, other steady-state configurations are also possible. In fact, with a simple extension of the above argument, as shown in Appendix B, one can derive the following more general result for a given fixed value of p (e.g., $p=\bar{p}$):

$$1=2C\frac{L}{L_A}\int_{-L_A/2L}^{+L_A/2L}d\eta\int_0^\infty d\rho\rho\chi'\frac{|A_{\bar{p}}|^2}{1+\Delta'^2+|A_{\bar{p}}f_{\bar{p}}|^2}\,, \tag{3.18a}$$

$$\delta\Omega'_{\bar{p}}=\frac{\kappa'}{1+\kappa'}\delta'_{AC}+\frac{\alpha'_1}{2\pi}\frac{\delta_{\bar{p}}}{1+\kappa'}\,, \tag{3.18b}$$

where α'_1 is the longitudinal mode spacing in units of $\gamma_\perp$ ($\alpha'_1=2\pi c/\Lambda\gamma_\perp$). The steady-state configuration corresponding to Eqs. (3.18) is also of the single-mode type; here the modal amplitudes $f_{p\neq\bar{p}}$ are vanishingly small in the uniform-field limit while $f_{\bar{p}}=O(1)$. Thus the solution of Eqs. (3.18) represent a stationary state corresponding to the modal configuration $A_{\bar{p}}$.

B. Discussion of the steady state

Equations (3.18) represent the main results of this section; together with Eqs. (3.9) they provide a complete specification of the steady state of a laser and its depen-

dence on the many physical and geometrical parameters of the model. We note that Eqs. (3.18) generalize the results of Ref. 24 and establish their domain of validity in more rigorous terms. The steady-state formula derived by Lugiato and Milani holds in the uniform-field limit for the $p=0$ mode and resonant operation. In addition, it requires a flat pump profile and a large Fresnel number. To establish the connection between these results in more explicit terms we note that if the length L_A of the medium is much smaller than the Rayleigh length $L\eta_0$, Eq. (3.17a) can be put in the approximate form

$$1=2C\frac{4}{\eta_0}\int_0^\infty d\rho\,\rho\frac{\exp\left[-\frac{\rho^2}{2\rho_p^2}\left[1+\frac{4\rho_p^2}{\eta_0}\right]\right]}{1+\frac{4|f_0|^2}{\eta_0}\exp\left[-\frac{2\rho^2}{\eta_0}\right]}, \tag{3.19}$$

and if $\rho_p/\sqrt{\eta_0}\gg 1$, Eq. (3.19) can be solved explicitly with the result

$$1=2C\frac{\eta_0}{4|f_0|^2}\ln\left[1+\frac{4|f_0|^2}{\eta_0}\right]. \tag{3.20}$$

This agrees with Eq. (4) of Ref. 24.

The integrals appearing in Eq. (3.18a) cannot be calculated in closed analytic form for arbitrary values of the parameters. It is not difficult, however, to calculate the threshold gain parameter for the $p=0$ mode using the pump profile (3.5). In fact, after setting $f_0=0$, Eq. (3.17) leads to

$$(2C)_{\rm thr}=(1+\Delta'^2)\frac{L_A}{L}\left[\tau_1\frac{2\eta_0\psi^2}{(1+\psi^2)^{1/2}}\tan^{-1}\left[\frac{L_A}{2L\eta_0(1+\psi^2)^{1/2}}\right]-\tau_2\frac{L_A}{L}\right]^{-1}, \tag{3.21}$$

where

$$\psi=\frac{2\rho_p}{\sqrt{\eta_0}}.$$

Equation (3.21) with $\tau_1=1$ and $\tau_2=0$ yields the threshold gain related to the pump profile (3.5b); with $\tau_1=2$ and $\tau_2=1$ we obtain the corresponding result for the pump distribution (3.5c).

An important design parameter is the ratio ψ between the pump waist ρ_p and the minimum beam size $\sqrt{\eta_0}$. It is clear by inspection that the threshold gain for laser action decreases as ψ increases, as it should be. The lowest threshold value corresponds to $\psi\to\infty$ and is given by the formula

$$(2C)_{\rm min,thr}=(1+\Delta'^2) \tag{3.22}$$

for both pump models (3.5).

The most obvious difference between the two pump profiles given by Eqs. (3.5) is the behavior of the threshold gain upon varying the parameter ψ. In the presence of an absorbing region ($\rho>\rho_p$) the threshold gain diverges for a finite critical value ψ_c such that the denominator in Eq. (3.21) vanishes. If instead the active medium is transparent at the edges of the pumped region, the threshold gain increases monotonically, and eventually diverges as ψ approaches zero. These considerations are summarized in Fig. 2 for typical values of η_0 and L_A/L. (Note that in order to avoid excessive repetitions of the parameters in the figure captions, most relevant values are tabulated in Table I; additional comments are enclosed in each figure caption, as needed.)

The behavior of the modal intensity as a function of the gain parameter allows some interesting observations but shows no major surprises. For example, we looked carefully for the possible presence of bistability near the threshold for laser action, as observed in some earlier experiments,[31] but found no evidence of this behavior. Some typical steady-state modal intensities are shown in Figs. 3 and 4 for a resonant and an off-resonant case. It is interesting to note that for increasing gain parameter, the modal intensity of the radial sidebands can exceed that of the $p=0$ mode. This effect is related to the different transverse profile of the various radial eigenfunctions and therefore is strictly a transverse effect. When the pumped region is sufficiently broader than the waist of the TEM_{00} mode, higher-order modes can take better advantage of the available gain because of their greater modal extent (see Fig. 3). The effect is enhanced in the presence of a detuning (Fig. 4) because of the increased coupling between the radial sidemodes and the atomic line. Figures 3 and 4 correspond to a pump profile of the type given by Eq. (3.5b) with a parameter $\psi=10$ (i.e., with a large pump

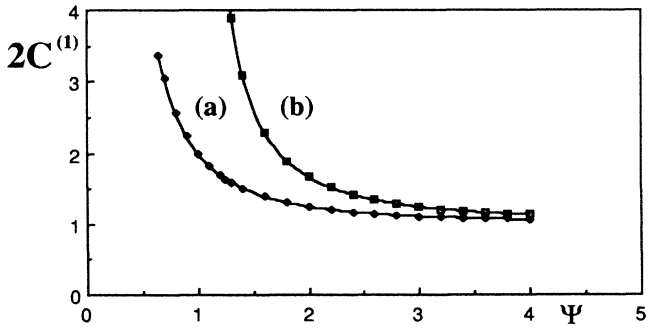

FIG. 2. Ordinary laser threshold gain $2C^{(1)}$ plotted as a function of the parameter $\psi=2\rho_P/\sqrt{\eta_0}$ for (*a*) a gain profile of the type given by Eq. (3.5b) and (*b*) for the gain profile of Eq. (3.5c). As expected, an increase in the transverse dimension of the excited volume leads to a lower threshold gain in both cases.

TABLE I. Values of the parameters used in the figures.

Parameter	Value	Location
$f=L/\Lambda$	0.2	All figures
L_A/L	0.2	All figures
R (reflectivity)	0.9	All figures
ρ_0 (scaled radius of curvature of the mirrors)	5.0	Figs. 2–5,7,9–11
	4.1	Fig. 6
	8.0	Figs. 12,13
α_1' (scaled free spectral range)	1.0	Figs. 2–6,12,13
	2.0	Fig. 7
	0.5	Fig. 11
	Variable	Figs. 9,10
δ'_{AC} (scaled detuning)	0.0	Figs. 2,3,5,6,9–11
	0.3	Fig. 4
	Variable	Figs. 7,12,13
$\sqrt{\eta_0}$ (beam waist)	2.14	Figs. 2–5,7,9–11
	3.36	Fig. 6
	1.99	Figs. 12,13
$\delta\omega_1'$ (scaled radial frequency spacing)	0.74	Figs. 2–5
	0.91	Fig. 6
	1.48	Fig. 7
	0.37	Fig. 11
	0.54	Figs. 12,13
	Variable	Figs. 9,10
$\psi=2\rho_P/\sqrt{\eta_0}$	10.0	Figs. 3,4,6,7,9–13
	1.7	Fig. 5
	Variable	Fig. 2

waist relative to the beam size). In this case one expects that the pump profile (3.5c) should yield rather similar results. Indeed the differences are small and only quantitative in character.

We also expect that the shape of the pump profile should play a more significant role when the ratio $2\rho_p/\sqrt{\eta_0}$ is closer to unity. A comparison between the steady-state curves obtained from Eq. (3.5b) with those resulting from Eq. (3.5c) is shown in Fig. 5. Here again the result is not surprising if we consider that in the latter case the presence of an absorbing ring around the edges of the medium is bound to affect the higher-order radial modes more than it affects the TEM_{00} configuration.

It is also interesting to note that the crossing of the modal intensity curves is a transverse effect which is less pronounced when the intensity profile of the beam becomes more homogeneous in the radial direction, i.e., when $\rho_p\sqrt{\eta_0}\gg 1$. An example is shown in Fig. 6 for a

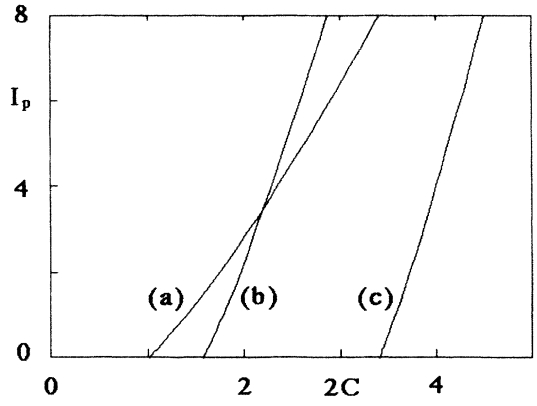

FIG. 3. Dependence of the steady-state output intensity (in arbitrary units) on the gain parameter $2C$ [Eq. (3.18a)] for (a) mode $p=0$, (b) mode $p=1$, (c) mode $p=2$. The gain profile of the medium corresponds to Eq. (3.5b). The larger output intensity acquired by mode $p=1$ relative to $p=0$ for $2C$ greater than about 2 is a consequence of the larger modal volume of the higher-order modes, which provides a better match with the pumped medium.

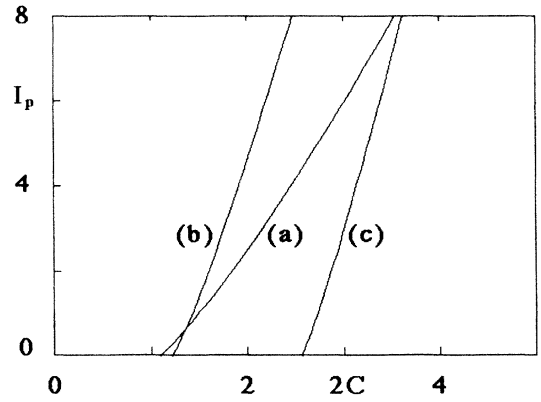

FIG. 4. Same as Fig. 3 but with a detuning parameter $\delta'_{AC}=0.3$ which is 30% of the chosen free spectral range ($\alpha_1'=1$) and almost one-half of the separation between adjacent radial modes ($\delta\omega_1'=0.74$).

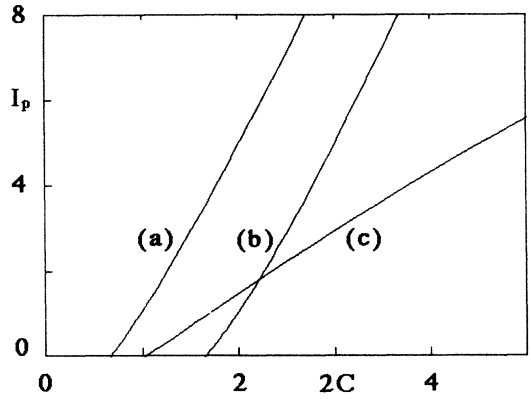

FIG. 5. Dependence of the steady-state output intensity on the gain parameter $2C$ [Eq. (3.18a)] for a medium characterized by the gain profile (3.5b) for curves (a) and (b), and by the profile (3.5c) for curve (c). Curves (a) and (b) correspond to $p=0$ and $p=1$, respectively; curve (c) corresponds to $p=0$. The chosen value of ψ ($\psi=1.7$) simulates a thin column of active medium. As expected, in this case the presence of an absorbing region at the radial edges causes a significant decrease in the output intensity of the $p=0$ mode (the curve for the mode $p=1$ is out of scale).

pump profile of the type (3.5b).

The dependence of the modal intensity on the detuning parameter δ'_{AC} is shown in Fig. 7 for a set of parameters where more than one transverse mode can be above threshold for the same value of δ'_{AC}. In general, this result does not imply that more than one mode will be above threshold at the same time because the presence of a given steady state alters the unsaturated gain distribution. Based on past experience with the plane-wave model[6(g)] we expect that modes $p=0$ and $p=1$, under the conditions of the figure, will compete and produce either

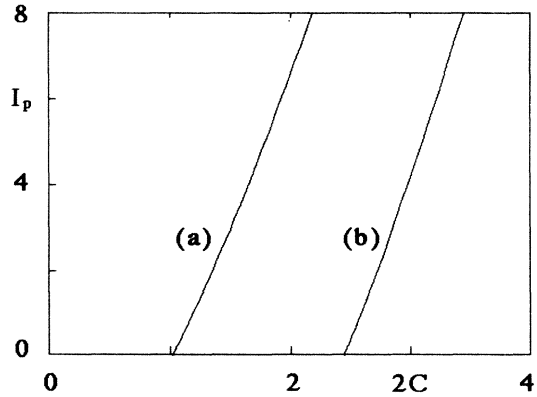

FIG. 6. The dependence of the output intensity on the gain approaches the qualitative behavior of the plane-wave theory when the transverse profile of the beam becomes more homogeneous in the radial direction. Here we have increased both the beam waist and the width of the pumped region relative, for example, to the values used in Fig. 4. Note, however, that the parameter ψ is the same as in Fig. 4 ($\psi=10$). The gain profile is given by Eq. (3.5b). Curve (a) corresponds to mode $p=0$; curve (b), to $p=1$.

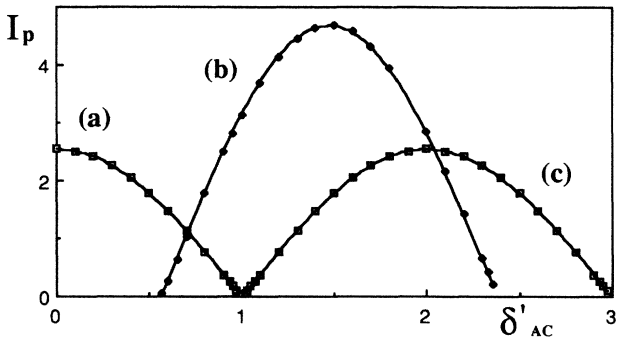

FIG. 7. Dependence of the modal intensity on the detuning parameter. Curve (a) shows the behavior of the mode ($\bar{n},p=0$), curve (b) corresponds to the mode ($\bar{n},p=1$), and curve (c) corresponds to ($\bar{n}+1,p=0$). Note that the free spectral range is $\alpha'_1=2$ and the separation between adjacent radial modes is $\delta\omega'_1=1.48$. The gain profile is given by Eq. (3.5b).

discontinuous jumps (mode hopping) or undamped pulsations through a mechanism that was identified as a phase instability in the plane-wave model. Naturally, this is a conjecture at this level; the issue can only be verified in the context of the linear-stability analysis, as we shall discuss in Sec. III. We conclude this section by noting the qualitatively similar behavior of the output intensity of a CO_2 laser during a detuning scan, as shown in Fig. 8.

IV. LINEAR-STABILITY ANALYSIS

The starting point of our analysis is the set of equations (3.8) for the modal amplitudes and for the atomic variables, together with the boundary conditions for the ring resonator. With the laser in a steady state we ask whether fluctuations corresponding to the modal indices (n,p) can grow exponentially out of noise. This is the usual picture behind the onset of unstable behavior. The real part of the rate constant for this process yields the rate of growth of the unstable modes, while the imaginary part measures the oscillation frequency resulting from the beat

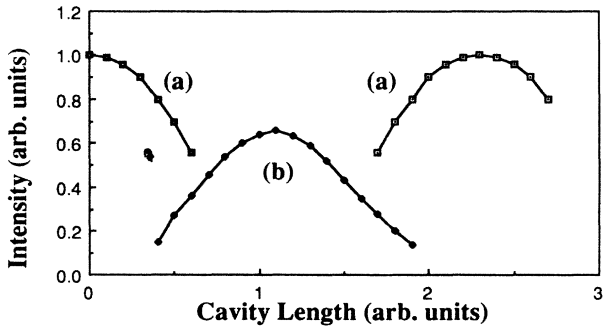

FIG. 8. Experimental output intensity of a conventional CO_2 laser as a function of the cavity length. Curves (a) correspond to the laser operating in two consecutive TEM_{00} modes and curve (b) to a TEM_{01+10} mode. Additional studies will be needed to determine if the observed bistability is the result of hysteresis in the piezoelectric ceramic driver of the cavity mirror, or if it is intrinsic to the dynamics of the system.

of the unstable mode and the steady-state field.

As our first step we map the coordinates η and τ into the new pair of independent variables η' and τ' according to the transformation

$$\eta'=\eta\ ,\qquad \tau'=\tau+\gamma_\perp\frac{\Lambda-L}{c}(\eta+\tfrac{1}{2})\ , \tag{4.1}$$

with the result that the new boundary conditions take on an isochronous form. Next, we linearize the equations of motion (3.8) and obtain

$$\frac{\partial\delta f_p}{\partial\eta'}+\frac{1}{v}\frac{\partial\delta f_p}{\partial\tau'}=i\frac{\delta\Omega'}{v}f_p-\alpha L\int_0^\infty d\rho\,\rho\,A_p^*(\rho,\eta)\delta\mathbf{P}\ , \tag{4.2a}$$

$$\frac{\partial\delta\mathbf{P}}{\partial\tau'}=-[\delta\mathbf{F}D_{\rm st}+\mathbf{F}_{\rm st}\delta D+(1+i\Delta')\delta\mathbf{P}]\ , \tag{4.2b}$$

$$\frac{\partial\delta D}{\partial\tau'}=-\gamma[-\tfrac{1}{2}(\delta\mathbf{F}^*\mathbf{P}_{\rm st}+\mathbf{F}_{\rm st}^*\delta\mathbf{P}+\text{c.c.})+\delta D]\ , \tag{4.2c}$$

where

$$\delta\mathbf{F}(\rho,\eta',\tau')=\sum_p A_p(\rho,\eta')\delta f_p(\eta',\tau')\ . \tag{4.3}$$

In addition, of course, one must also include linearized equations for δf_p^* and $\delta\mathbf{P}^*$, which are complex conjugates of Eqs. (4.2a) and (4.2b), respectively. The boundary conditions are

$$\delta f_p(-1/2,\tau')=Re^{-i\delta_p}\exp\left[i\delta\Omega'\gamma_\perp\frac{\Lambda-L}{c}\right]\times\delta f_p(1/2,\tau')\ , \tag{4.4}$$

as one can verify at once using Eq. (3.8d) in the new reference frame.

Following the standard procedure we introduce the ansatz

$$\begin{bmatrix}\delta f_p(\eta',\tau')\\ \delta f_p^*(\eta',\tau')\\ \delta\mathbf{P}(\rho,\eta',\tau')\\ \delta\mathbf{P}^*(\rho,\eta',\tau')\\ \delta D(\rho,\eta',\tau')\end{bmatrix}=e^{\lambda\tau'}\begin{bmatrix}\delta\varphi_p(\eta')\\ \delta\varphi_p^*(\eta')\\ \delta p(\rho,\eta')\\ \delta p^*(\rho,\eta')\\ \delta d(\rho,\eta')\end{bmatrix} \tag{4.5}$$

in the linearized equations (4.2); λ denotes the linearized rate constant in units of $\gamma_\perp$. The equations for the atomic fluctuation variables are algebraic in nature and can be solved at once with the result

$$\delta p(\rho,\eta')=T_1(\rho,\eta',\lambda)\sum_{p'}A_{p'}(\rho,\eta')\delta\varphi_{p'}(\eta')+T_2(\rho,\eta',\lambda)\sum_{p'}A_{p'}^*(\rho,\eta')\delta\varphi_{p'}^*(\eta')\ , \tag{4.6a}$$

$$\delta p^*(\rho,\eta')=T_2^*(\rho,\eta',\lambda)\sum_{p'}A_{p'}(\rho,\eta')\delta\varphi_{p'}(\eta')+T_1^*(\rho,\eta',\lambda)\sum_{p'}A_{p'}^*(\rho,\eta')\delta\varphi_{p'}^*(\eta')\ , \tag{4.6b}$$

where

$$T_1=\frac{c_3c_1^*-c_2c_4^*}{c_1c_1^*-c_2c_2^*}\ , \tag{4.7a}$$

$$T_2=\frac{c_4c_1^*-c_2c_3^*}{c_1c_1^*-c_2c_2^*}\ , \tag{4.7b}$$

and

$$c_1(\rho,\eta')=\lambda+1+i\Delta'+\frac{1}{2}\frac{\gamma}{\lambda+\gamma}|\,\mathbf{F}_{\rm st}\,|^2\ , \tag{4.8a}$$

$$c_2(\rho,\eta')=\frac{1}{2}\frac{\gamma}{\lambda+\gamma}\mathbf{F}_{\rm st}^2\ , \tag{4.8b}$$

$$c_3(\rho,\eta')=-\left[D_{\rm st}+\frac{1}{2}\frac{\gamma}{\lambda+\gamma}\mathbf{F}_{\rm st}\mathbf{P}_{\rm st}^*\right]\ , \tag{4.8c}$$

$$c_4(\rho,\eta')=-\frac{1}{2}\frac{\gamma}{\lambda+\gamma}\mathbf{F}_{\rm st}\mathbf{P}_{\rm st}\ . \tag{4.8d}$$

The symbols c_1^*,c_2^*, etc. indicate the complex-conjugate parameters of c_1 and c_2, etc.; we note, however, that in performing the complex-conjugate operation we must handle λ as if it were a real variable, i.e., c_i^* is a function of λ and not λ^*. The reason for this peculiar rule can be traced back easily to the equations of motion for δp and δp^* and to the ansatz (4.5).

At this point the linearized field equations become

$$\frac{\partial\delta\varphi_p}{\partial\eta'}+\gamma_\perp\frac{\Lambda}{c}\lambda\delta\varphi_p=i\frac{\delta\Omega'}{v}\delta\varphi_p-\alpha L\int_0^\infty d\rho\,\rho\,A_p^*(\rho,\eta')\left[T_1(\rho,\eta',\lambda)\sum_{p'}A_{p'}(\rho,\eta')\delta\varphi_{p'}(\eta')+T_2(\rho,\eta',\lambda)\sum_{p'}A_{p'}^*(\rho,\eta')\delta\varphi_{p'}^*(\eta')\right]\ , \tag{4.9a}$$

$$\frac{\partial\delta\varphi_p^*}{\partial\eta'}+\gamma_\perp\frac{\Lambda}{c}\lambda\delta\varphi_p^*=-i\frac{\delta\Omega'}{v}\delta\varphi_p^*-\alpha L\int_0^\infty d\rho\,\rho\,A_\pi(\rho,\eta')\left[T_2^*(\rho,\eta',\lambda)\sum_{p'}A_{p'}(\rho,\eta')\delta\varphi_{p'}(\eta')+T_1^*(\rho,\eta',\lambda)\sum_{p'}A_{p'}^*(\rho,\eta')\delta\varphi_{p'}^*(\eta')\right]\ . \tag{4.9b}$$

The appropriate boundary conditions take the form

$$\delta\varphi_p(-1/2)=Re^{-i\delta_p'}\delta\varphi_p(1/2)\ , \tag{4.9c}$$

where

$$\delta'_p=\delta_p-\delta\Omega'\gamma_\perp\frac{\Lambda-L}{c} . \tag{4.10}$$

Before taking the final steps with the calculation of the linearized eigenvalues it is convenient to introduce one more change of dependent variables, whose main purpose is to transform the boundary conditions to a standard periodicity form. This can be accomplished with the definitions

$$\delta\varphi_p(\eta')=v_p(\eta')\exp\{-(\eta'+\tfrac{1}{2})[(\ln R)-i\delta'_p]\} , \tag{4.11a}$$

$$\delta\varphi_p^*(\eta')=v_p^*(\eta')\exp\{-(\eta'+\tfrac{1}{2})[(\ln R)+i\delta'_p)]\} \tag{4.11b}$$

because, as we can easily see with the help of Eqs. (4.9c) and (4.11), we have

$$v_p(-1/2)=v_p(1/2) , \tag{4.12a}$$

$$v_p^*(-1/2)=v_p^*(1/2) . \tag{4.12b}$$

The transformed field fluctuation equations take the form

$$\begin{aligned}&\frac{c}{\Lambda\gamma_\perp}\frac{\partial v_p}{\partial\eta'}+\left[\kappa'+i\frac{c}{\Lambda\gamma_\perp}\delta_p-i\delta\Omega'\right]v_p+\lambda v_p\\&=-\kappa' 2C\frac{L}{L_A}\int_0^\infty d\rho\,\rho\,A_p^*(\rho,\eta')\left[T_1(\rho,\eta',\lambda)\sum_{p'}A_{p'}(\rho,\eta')v_{p'}(\eta')\exp[i(\eta'+\tfrac{1}{2})(\delta'_{p'}-\delta'_p)]\right.\\&\left.+T_2(\rho,\eta',\lambda)\sum_{p'}A_{p'}^*(\rho,\eta')v_{p'}(\eta')\exp[-i(\eta'+\tfrac{1}{2})(\delta'_{p'}+\delta'_p)]\right] ,\end{aligned} \tag{4.13}$$

with a similar equation for v_p^* following from the complex conjugation of (4.13).

The required linearized eigenvalues cannot be calculated in closed form for arbitrary values of the parameters in spite of the linear nature of Eq. (4.13) and its complex conjugate. However, in the good cavity limit $\kappa'\ll 1$, it is possible to develop a perturbative procedure whose end result is the analytic derivation of the instability condition. Numerical calculations are needed only to carry out the quadrature of the final integral expression. Our strategy can be summarized as follows. By taking advantage of the periodic nature of the boundary conditions (4.12) we expand v_p and v_p^* in appropriate Fourier series over the interval $-\frac{1}{2}\le\eta'\le\frac{1}{2}$ according to the usual relations

$$v_p=\sum_n e^{ik_nL\eta'}\sigma_{n,p} , \tag{4.14a}$$

$$v_p^*=\sum_n e^{-ik_nL\eta'}\sigma_{n,p}^* , \tag{4.14b}$$

where $k_n=2\pi n/L$ ($n=0,\pm1,\pm2,\ldots$), and $\sigma_{n,p}$ and $\sigma_{n,p}^*$ are complex coefficients. Next we construct an algebraic system of equations for the fluctuation amplitudes $\sigma_{n,p}$ and $\sigma_{n,p}^*$ with the help of the orthonormality relation

$$\int_{-1/2}^{1/2}d\eta' e^{ik_nL\eta'}e^{-ik_mL\eta'}=\delta_{n,m} . \tag{4.15}$$

Finally, we only need to solve the resulting linear algebraic problem to first order in κ'.

Application of Eqs. (4.14) and (4.15) leads to

$$\begin{aligned}&i\alpha'_n\sigma_{n,p}+\left[\kappa'+i\frac{c}{\Lambda\gamma_\perp}\delta_p-i\delta\Omega'\right]\sigma_{n,p}+\lambda\sigma_{n,p}\\&=\kappa'\sum_{n',p'}[\Phi_{n,p}^{n',p'}(\lambda)\sigma_{n',p'}+\Psi_{n,p}^{n',p'}(\lambda)\sigma_{n',p'}^*] ,\end{aligned} \tag{4.16a}$$

$$\begin{aligned}&-i\alpha'_n\sigma_{n,p}^*+\left[\kappa'-i\frac{c}{\Lambda\gamma_\perp}\delta_p+i\delta\Omega'\right]\sigma_{n,p}^*+\lambda\sigma_{n,p}^*\\&=\kappa'\sum_{n',p'}[\Phi_{n,p}^{n',p'*}(\lambda)\sigma_{n',p'}^*+\Psi_{n,p}^{n',p'*}(\lambda)\sigma_{n',p'}] ,\end{aligned} \tag{4.16b}$$

where

$$\alpha'_n=n\alpha'_1=\frac{2\pi nc}{\Lambda\gamma_\perp}$$

is the frequency separation between the nth longitudinal resonance and the reference frequency measured in units of $\gamma_\perp$, and the coefficients Φ and Ψ are defined by

$$\Phi_{n,p}^{n',p'}(\lambda)=-2C\frac{L}{L_A}\int_{-L_A/2L}^{+L_A/2L}d\eta' e^{i(k_{n'}-k_n)L\eta'}e^{i(\eta'+\frac{1}{2})(\delta'_{p'}-\delta'_p)}\int_0^\infty d\rho\,\rho\,A_p^*(\rho,\eta')A_{p'}(\rho,\eta')T_1(\rho,\eta',\lambda) , \tag{4.17a}$$

$$\Psi_{n,p}^{n',p'}(\lambda)=-2C\frac{L}{L_A}\int_{-L_A/2L}^{+L_A/2L}d\eta' e^{-i(k_{n'}+k_n)L\eta'}e^{i(\eta'+\frac{1}{2})(\delta'_{p'}+\delta'_p)}\int_0^\infty d\rho\,\rho\,A_p^*(\rho,\eta')A_{p'}^*(\rho,\eta')T_2(\rho,\eta',\lambda) . \tag{4.17b}$$

The solution of Eqs. (4.16) is equivalent to the diagonalization of the problem

$$L\vec{v}=\lambda\vec{v}\ , \tag{4.18}$$

where the matrix L, whose definition is obvious from Eqs. (4.16), has the structure

$$L=L_0+\kappa' L_1\ , \tag{4.19}$$

and $\vec{v}$ is the column vector with components $\sigma_{n,p}$ and $\sigma^*_{n,p}$. Now we assume the good cavity condition $\kappa'\ll 1$ and proceed to evaluate the eigenvalues to first order in κ'. We assume also that the longitudinal mode spacing $\alpha_1=2\pi c/\Lambda$ and the atomic linewidth $\gamma_\perp$ are of the same order of magnitude. Hence the good cavity condition

$$\kappa'=\left[\frac{\alpha_1}{2\pi\gamma_\perp}\right]T\ll 1$$

is equivalent to the uniform-field condition $T\ll 1$.

We consider now the stationary solution

$$\mathbf{F}_{\rm st}(\rho,\eta')=A_0(\rho,\eta')f_0 \tag{4.20}$$

for which $\delta\Omega'$ is of the order of κ'. We select two values of the indices n and p (say, $\bar{n}$ and $\bar{p}$).

(a) Consider first the case $\bar{p}\neq 0$, and assume that there be no accidental degeneracy of the type

$$\alpha'_{\bar{n}}+\frac{c}{\Lambda\gamma_\perp}\delta_{\bar{p}}\pm\left[\alpha'_n+\frac{c}{\Lambda\gamma_\perp}\delta_n\right]=0(\kappa') \tag{4.21}$$

for any n and p other than the chosen $\bar{n}$ and $\bar{p}$. Under this condition the eigenstates of L have the form

$$\sigma_{\bar{n},\bar{p}}=\sigma^{(0)}_{\bar{n},\bar{p}}+O(\kappa')=\sigma^{(0)}_{\bar{n},\bar{p}}+\kappa'\sigma^{(1)}_{\bar{n},\bar{p}} \tag{4.22a}$$

and

$$\sigma_{n,p}=O(\kappa')\ , \tag{4.22b}$$

$$\sigma^*_{n,p}=O(\kappa')\ . \tag{4.22c}$$

Equations (4.22b) and (4.22c) apply to $n,p\neq\bar{n},\bar{p}$. Consider now Eq. (4.16a) with $n,p=\bar{n},\bar{p}$ and let

$$\lambda=\lambda^{(0)}+\kappa'\lambda^{(1)}=-i\left[\alpha'_{\bar{n}}+\frac{c}{\Lambda\gamma_\perp}\delta_{\bar{p}}\right]+\kappa'\lambda^{(1)}\ . \tag{4.23}$$

After substitution of Eqs. (4.22) and (4.23) into Eq. (4.16a) we obtain

$$-i\left[\alpha'_{\bar{n}}+\frac{c}{\Lambda\gamma_\perp}\delta_{\bar{p}}\right]\sigma^{(0)}_{\bar{n},\bar{p}}=\lambda^{(0)}\sigma^{(0)}_{\bar{n},\bar{p}} \tag{4.24a}$$

and

$$\lambda^{(1)}=-1+i\frac{\delta\Omega'}{\kappa'}+\Phi^{\bar{n},\bar{p}}_{\bar{n},\bar{p}}(\lambda^{(0)})\ , \tag{4.24b}$$

where

$$\Phi^{\bar{n},\bar{p}}_{\bar{n},\bar{p}}(\lambda^{(0)})=-2C\frac{L}{L_A}\int_{-L_A/2L}^{+L_A/2L}d\eta'\int_0^\infty d\rho\,\rho\,|\,A_{\bar{p}}(\rho,\eta')\,|^2\times T_1(\rho,\eta',\lambda^{(0)})\ . \tag{4.24c}$$

Equation (4.24a) gives the nondegenerate lowest-order eigenvalues, while (4.24b) gives their first-order corrections.

(b) Consider now the case $\bar{p}=0$. We note that the eigenvalue

$$\lambda^{(0)}=-i\alpha'_{\bar{n}}$$

is doubly degenerate, as we can easily confirm by considering Eq. (4.16a) for $\sigma_{\bar{n},0}$ and Eq. (4.16b) for $\sigma^*_{-\bar{n},0}$. It follows that the corresponding eigenvalues are of the form

$$\sigma_{\bar{n},0}=\sigma^{(0)}_{\bar{n},0}+O(\kappa')\ , \tag{4.25a}$$

$$\sigma^*_{-\bar{n},0}=(\sigma^{*(0)}_{-\bar{n},0})+O(\kappa')\ , \tag{4.25b}$$

$$\sigma_{n,p}=O(\kappa')\ \text{ for } n,p\neq\bar{n},0\ , \tag{4.25c}$$

$$\sigma^*_{n,p}=O(\kappa')\ \text{ for } n,p\neq-\bar{n},0\ . \tag{4.25d}$$

If we now set $(n,p)=(\bar{n},0)$ in Eq. (4.16a), and $(n,p)=(-\bar{n},0)$ in Eq. (4.16b), and equate the first-order terms in κ', we obtain

$$(1+\lambda^{(1)})\sigma^{(0)}_{\bar{n},0}=\Phi^{\bar{n},0}_{\bar{n},0}(\lambda^{(0)})\sigma^{(0)}_{\bar{n},0}+\Psi^{-\bar{n},0}_{-\bar{n},0}(\lambda^{(0)})\sigma^{*(0)}_{-\bar{n},0}\ , \tag{4.26a}$$

$$(1+\lambda^{(1)})\sigma^{*(0)}_{-\bar{n},0}=\Phi^{-\bar{n},0*}_{-\bar{n},0}(\lambda^{(0)})\sigma^{*(0)}_{-\bar{n},0}=\Psi^{\bar{n},0}_{\bar{n},0}(\lambda^{(0)})\sigma^{(0)}_{\bar{n},0}\ . \tag{4.26b}$$

These equations lead to the first-order corrections $\lambda^{(1)}$ of the eigenvalues in the degenerate case. In particular, in the limit $L_A\ll L\eta_0$ and in resonance ($\delta'_{AC}=0$), we find the results already obtained by Lugiato and Milani.[24]

If the stationary state is of the type

$$\mathbf{F}_{\rm st}(\rho,\eta')=A_q(\rho,\eta')f_q \tag{4.27}$$

corresponding to a single radial mode q, the above treatment needs only a few simple modifications. Equations (4.16) still hold with $\delta\Omega'$ replaced by $\delta\Omega'_q$. The frequency offset $\delta\Omega'_q$ given by Eq. (3.18b) contains a large contribution and a correction of order κ'. The unperturbed eigenvalues [Eq. (4.24a)] contain only the large contributions and are given by

$$\lambda^{(0)}_{n,p}=-i\left[\alpha'_n+\frac{c}{\Lambda\gamma_\perp}(\delta_p-\delta_q)\right]\ , \tag{4.28}$$

and of course the symbol $\lambda^{(0)}$ that appears in Eqs. (4.24b) and (4.26) must be interpreted according to Eq. (4.28).

Now we consider the linearized stability problem in the full adiabatic elimination regime of the atomic variables (i.e., when $\gamma_\perp,\gamma_\parallel\gg c/\Lambda$). Here again the general procedure needs only a few minor modifications in order to fit the limiting situation. In fact, with reference to Eqs. (4.2b) and (4.2c), the adiabatic elimination limit corresponds to setting both time derivatives equal to zero. In this case the resulting expressions given by Eqs. (4.8) remain valid provided we set $\lambda=0$. Thus the linearized eigenvalues in this limit are still given by Eqs. (4.24b) and (4.26) with $\lambda^{(0)}$ formally equal to zero and T_1 and T_2 given by the simple formulas

$$T_1(\rho,\eta')=-\chi'(\rho)\frac{(1+\Delta'^2)(1-i\Delta')}{(1+\Delta'^2+|\mathbf{F}_{st}|^2)^2}\ , \tag{4.29a}$$

$$T_2(\rho,\eta')=\chi'(\rho)\frac{(1-i\Delta')\mathbf{F}_{st}^2}{(1+\Delta'^2+|\mathbf{F}_{st}|^2)^2}\ . \tag{4.29b}$$

In this case $\lambda^{(1)}$ depends on $\bar{p}$ only by way of the modal function $|A_{\bar{p}}|^2$, while away from the adiabatic regime it depends on the radial index also through the unperturbed frequency

$$\lambda_{\bar{p}}^{(0)}=-i\left[\alpha'_{\bar{n}}+\frac{c}{\Lambda\gamma_\perp}\delta_{\bar{p}}\right]\ .$$

Another interesting limit is one in which the length L_A of the atomic sample is much smaller than the Rayleigh length $L\eta_0$. In this case Eq. (4.24c) reduces to

$$\Phi_{\bar{n},\bar{p}}^{\bar{n},\bar{p}}(\lambda^{(0)})=-2C\frac{4}{\eta_0}\int_0^\infty d\rho\,\rho\exp\left[-\frac{2\rho^2}{\eta_0}\right]L_{\bar{p}}^2\left[\frac{2\rho^2}{\eta_0}\right]\times T_1(\rho,\eta',\lambda^{(0)})\ , \tag{4.30}$$

and in the expression for T_1 given by Eqs. (4.7a) and (4.8) one must replace $|\mathbf{F}_{st}|^2$ with the expression

$$|\mathbf{F}_{st}|^2=\frac{4}{\eta_0}\exp\left[-\frac{2\rho^2}{\eta_0}\right]L_q^2\left[\frac{2\rho^2}{\eta_0}\right]f_q\ . \tag{4.31}$$

It is important to remark that the gain parameter C in Eq. (4.24c) is related to the amplitude $f_{\bar{p}}$ of the stationary field, which appears in T_1 through $\mathbf{F}_{st}$, by the state equation (3.18). In addition, we note that for correctness, the expression for Δ' which is needed in calculating T_1 should be evaluated to order zero in κ'. Finally, because $\lambda^{(0)}$ is a pure imaginary number, the instability condition is given by the equation

$$\mathrm{Re}\lambda^{(1)}>0\ . \tag{4.32}$$

V. STABILITY ANALYSIS: NUMERICAL RESULTS

The main results of Sec. IV can be summarized as follows.

(i) In the extended uniform-field limit (3.12a) and (3.12b) with α_1 and $\gamma_\perp$ of the same order of magnitude, a single-mode steady-state field characterized by modal indices $\bar{n}$ and $\bar{p}$ becomes unstable if

$$\mathrm{Re}\lambda_{n,p}^{(1)}>0 \tag{5.1}$$

for at least a pair of values of the indices n and p.

(ii) If $p\neq\bar{p}$, Eq. (5.1) takes the explicit form

$$-1+\mathrm{Re}\Phi_{n,p}^{n,p}(\lambda^{(0)})>1\ , \tag{5.2}$$

where

$$\Phi_{n,p}^{n,p}(\lambda^{(0)})=-2C\frac{L}{L_A}\int_{-L_A/2L}^{L_A/2L}d\eta'\int_0^\infty d\rho\,\rho\,|A_p(\rho,\eta')|^2\times T_1(\rho,\eta',\lambda^{(0)})\ , \tag{5.3}$$

$$\lambda^{(0)}=-i\left[\alpha'_n+\frac{c}{\Lambda\gamma_\perp}\delta_p\right]\ , \tag{5.4}$$

and the function T_1 is defined by Eqs. (4.7) and (4.8).

(iii) If $p=\bar{p}$, $\lambda^{(1)}$ is the solution of the quadratic equation that results from the linear homogeneous system (4.25).

(iv) The instability threshold for the mode with indices n and p, also known as the second laser threshold, is the value of $2C$ that satisfies the identity

$$-1+\mathrm{Re}\Phi_{n,p}^{n,p}(\lambda^{(0)})=1\ . \tag{5.5}$$

To avoid confusion between this threshold value and the threshold for ordinary laser action, we denote the former by $2C^{(2)}$ and the latter by $2C^{(1)}$.

The parameter space is much wider than in the case of the usual plane-wave theory. Numerous geometrical and physical parameters play an important role in providing the conditions for unstable behavior so that a complete scan of the relevant space is a monumental task. Here, in an attempt to aid our analysis and to provide some guidelines for future searches, we have identified the parameters that can be viewed as independent of one another, at least from a theoretical standpoint. For the general detuned case, i.e., when $\delta'_{AB}\neq 0$, these are listed in Table II. In the resonant case, and with the additional restriction that the steady-state field is of the TEM_{00} type, the independent parameters are $2C$, η_0, $\psi=\rho_P/\sqrt{\eta_0}$, $\delta\omega'_1$, γ, and L_A/L; note that $\delta\omega'_1=\delta_1\alpha'_1/2\pi$.

The numerical results collected in this section represent a typical cross section of data that we have calculated in a fairly-large-size (but definitely not exhaustive) scan of the parameter space. Undoubtedly, additional useful facts will emerge from future studies. For convenience we have divided our survey into two sections. The first relates to a resonant laser ($\delta'_{AC}=0$), the second to a detuned situation.

A. Resonant lasers

The instability threshold is rather sensitive to the cavity geometry. In fact, the second laser threshold is a monotonic function of the transverse mode spacing, as shown in Fig. 9, where we display this dependence for three values of γ. On the basis of this result one can infer that long resonators or cavities whose curved mirrors have large radii of curvature should be more sensitive to instabilities even in the vicinity of the threshold for laser action. In addition, active media with a slow rate of population decay, relative to the decay of the polarization, are more unstable than those with comparable rates of decay for the population and the polarization. This behavior is quite different from what is predicted by the plane-wave theory where the axial mode spacing has very little influence on the value of the instability threshold.[6(e)]

As expected, if the laser operates in a TEM_{00} configuration the first radial sideband ($p=1$) is more likely to become unstable than the higher-order radial sidemodes ($p=2,3,\ldots$); this is illustrated in Fig. 10. The reduced influence of the higher-order transverse modes on the unstable dynamics is linked to their pro-

TABLE II. Independent parameters for the general detuned case.

Symbol	Meaning
$2C$	Unsaturated gain parameter
δ'_{AC}	Difference between the atomic transition frequency and the reference cavity resonance in units of $\gamma_\perp$
η_0	Rayleigh range of the field profile between the curved mirrors
$\psi=2\rho_P/\sqrt{\eta_0}$	Ratio between the waist of the pump medium and the beam waist in the region between the curved mirrors
$\delta\omega'_1$	Separation between the $(n,1)$ and the $(n,0)$ cavity resonances in units of $\gamma_\perp$
α'_1	Cavity free spectral range
R	Power reflectivity coefficient of the curved mirrors
γ	Ratio between the population and polarization relaxation rates
L_A/L	Ratio between the length of the active medium and the distance between the curved mirrors

gressively larger cross section, which causes the cavity field to see a smaller unsaturated gain because the equilibrium population difference χ' tapers radially out in a preassigned way. Furthermore, in practical devices, intracavity apertures provide an even more stringent selection mechanism by increasing the losses experienced by the higher-order modes to the point that they can no longer meet the ordinary threshold condition.

One of the key parameters that controls the appearance of low threshold instabilities is the ratio between the transverse size of the active volume and the beam cross section. Figure 11 shows the large drop of the instability threshold that accompanies an increase in the parameter ψ for both modes $p=1$ and $p=2$. Figure 11(a) corresponds to the pump model (3.5b), while Fig. 11(b) corresponds to (3.5c). This behavior is consistent with the results already shown in the previous figures so that again, for example, mode $p=2$ tends to be more stable than mode $p=1$. Furthermore, the presence of an absorbing region at the radial edges of the active medium [Fig. 11(b)] causes a lowering of the effective ratio between the transverse size of the gain volume and the beam waist; hence, the stability of the system is enhanced in the case shown in Fig. 11(b) relative to that of Fig. 11(a).

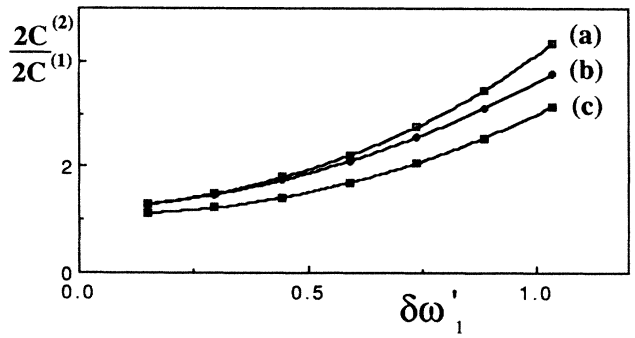

FIG. 9. Dependence of the second laser threshold $2C^{(2)}$ on the separation between adjacent radial modes for (*a*) $\gamma=2$, (*b*) $\gamma=1$, and (*c*) $\gamma=0.1$. The gain required to produce an instability of the $p=1$ mode in the presence of a $p=0$ steady state is measured in units of the ordinary threshold gain. Note that in all cases shown here the instability threshold is only slightly higher than the first laser threshold ($2C^{(2)}/2C^{(1)}$ is close to unity) when the separation between radial modes becomes progressively smaller. The gain profile is given by Eq. (3.5b).

B. Detuned laser

The effect of detuning is rather interesting also, although as indicated in Table I, a complete survey of the various possibilities will require a much more extensive study than we have carried out thus far. Figure 12 contains a composite map of the instability threshold values plotted as functions of the detuning parameter δ'_{AC} for four different off-resonant modes, under the assumption that the steady state of the laser is characterized by the modal indices $(\bar{n},0)$. The transverse modes $(\bar{n},1)$ and $(\bar{n},2)$ exhibit the same relative stability properties as displayed in previous figures, with mode $(\bar{n},2)$ always being more stable than mode $(\bar{n},1)$. This figure shows also that transverse modes belonging to the nearest longitudinal mode $(\bar{n}-1)$ can play an important role in the dynamics of this system. For the chosen values of the parameters the resonances of the modes $(\bar{n}-1,1)$ and

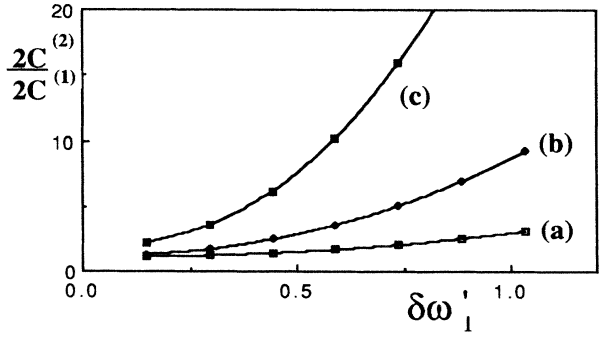

FIG. 10. Dependence of the second laser threshold $2C^{(2)}$ on the radial mode spacing $\delta\omega'_1$ for (*a*) $p=1$, (*b*) $p=2$, and (*c*) $p=3$. As expected, the lowest radial modes are the most sensitive to the appearance of unstable behavior. The gain profile is given by Eq. (3.5b).

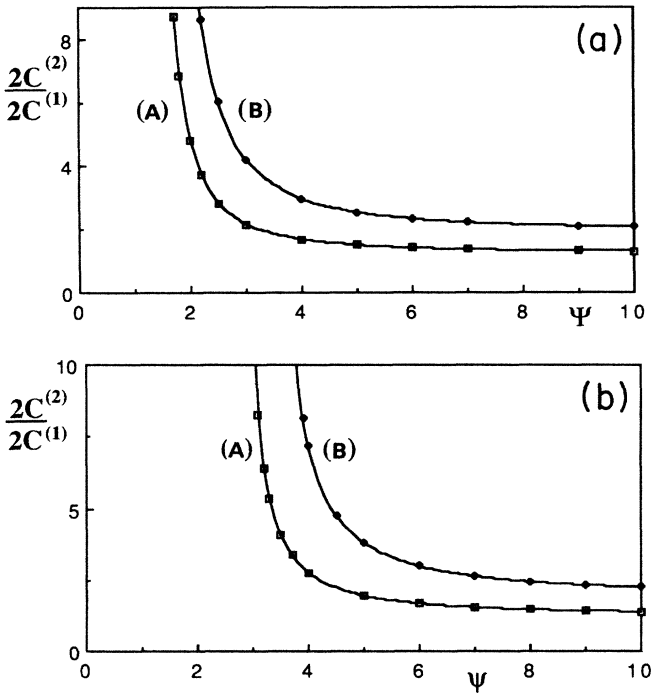

FIG. 11. (a) Dependence of the second laser threshold $2C^{(2)}$ on the parameter $\psi=2\rho_P/\sqrt{\eta_0}$ for (A) $p=1$ and (B) $p=2$. The pump profile corresponds to Eq. (3.5b). (b) Same as Fig. (a), with the pump profile given by Eq. (3.5c). These results show that the instability is favored when the cavity is designed to operate with a large value of the parameter ψ.

$(\bar{n}-1,2)$ are clustered around the resonant mode and can easily become unstable as we vary the detuning parameter. Mode $(\bar{n}-1,2)$, in particular, happens to fall in the vicinity of the resonant mode and has a low instability threshold for a fairly wide range of the detuning parameter. We recall, however, that in real laser systems the losses of higher-order transverse modes are higher than those of lower-order modes, so that in practice, the resonances characterized by an index p equal to or greater than 2 are likely to have no significant dynamical influence.

In an earlier paper dealing with the role of the Gaussian transverse profile on the dynamics of a ring laser, Lugiato and Milani[24] proposed the surprising result that the Risken-Nummedal[6(b),6(c)] instability disappears if every field mode has a TEM_{00} structure. Their calculation envisioned a ring laser operating in resonance and explored the possible existence of unstable axial modes with a different value of the longitudinal index. After assuming a flat pump profile (this gives the best chance for the development of an instability, as shown by our Fig. 11) they concluded that no longitudinal sidebands would ever be unstable.

If we consider that the theoretical threshold values for a Risken-Nummedal plane-wave instability are already unreasonably high, this result is very surprising because it suggests that transverse effects have a stabilizing action on laser dynamics. We confirm the results of Ref. 24 in Fig. 13. In fact, on resonance $(\delta'_{AC}=0)$, the sidemode $(\bar{n}+1,0)$ is indeed stable for all values of the gain (the same conclusion holds for all other TEM_{00} modes). It becomes unstable, instead, for sufficiently large values of the detuning parameter, as anticipated in Ref. 32, following a pattern that is typical of the so-called phase instability of the plane-wave theory.[6(g)] In the context of our formulation we cannot introduce a clear-cut discrimination between instabilities of the amplitude and phase-type because of the nature of the linearized spectrum of eigenvalues.[33] However, the behavior displayed in Fig. 13 is very reminiscent of the latter type of instability.

The combined message of our results is that the transverse profile of the field and of the atomic variables does play an important role in the emergence of low threshold instabilities, but the radial modes with the same longitudinal label as the operating steady state of the laser are the ones that are most closely responsible for introducing output pulsations.

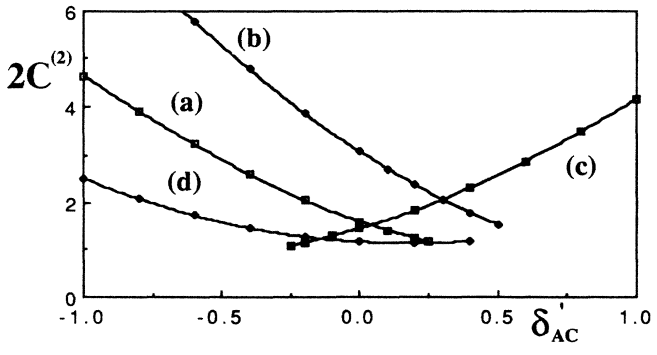

FIG. 12. Dependence of the second laser threshold $2C^{(2)}$ on the detuning parameter for a number of radial modes: (a) corresponds to $(\bar{n},p=1)$, (b) to $(\bar{n},p=2)$, (c) to $(\bar{n}-1,p=1)$, and (d) to $(\bar{n}-1,p=2)$. The pump profile is given by Eq. (3.5b).

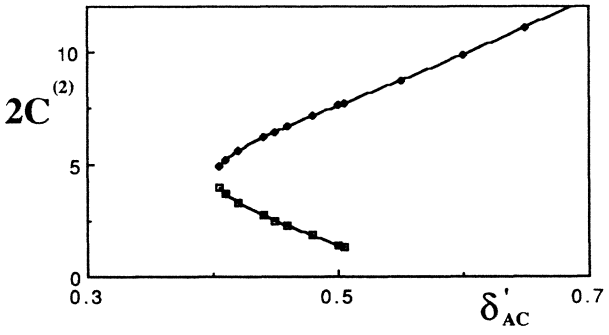

FIG. 13. Instability domain (to the right of the solid line) for the radial mode $(\bar{n}+1,p=0)$. As shown analytically in Ref. 24, this radial mode cannot become unstable under resonant conditions. For sufficiently large values of δ'_{AC} and appropriate values of the gain parameter, this radial mode becomes unstable through a mechanism that is reminiscent of a phase instability.

VI. CONCLUSION AND COMMENTS

With a suitable extension of the uniform-field limit [Eq. (3.12)] we have succeeded in carrying out a detailed analytical study of the steady-state and linear-stability properties of a ring laser containing a homogeneously broadened active medium. In this limited context we have been able to incorporate the effects of curved reflecting surfaces and the possible lack of transverse uniformity of the pump. The main claim of this paper is that these transverse effects can account, at least in good measure, for the emergence of low threshold unstable behavior.

We have identified the most critical parameters that affect the stability of this system. According to our results, instabilities are enhanced by a flat pump profile relative to the transverse shape of the field. To be more precise we found that if the ratio $2\rho_P/\sqrt{\eta_0}$ becomes sufficiently large, the threshold for instability decreases dramatically and can be only a few percent higher than the ordinary laser threshold. This is probably one of the most specific signs of the transverse instability. In fact, longitudinal instabilities are favored in the limiting configuration $\rho_P/\sqrt{\eta_0}\to 0$ with very large values of the gain parameter C,[17(e),24] while the transverse instabilities acquire a dominant role in the opposite limit ($\rho_P/\sqrt{\eta_0}\to\infty$ with a small value of C). In this sense we can distinguish between longitudinal and transverse instabilities. The former type is, of course, a high threshold phenomenon.

As already mentioned, each transverse mode with $p\neq 0$ is associated with only one eigenvalue, in contrast with the situation that prevails in the plane-wave theory where two linearized eigenvalues exist for each value of the longitudinal index n. This precludes a straightforward distinction between amplitude and phase instabilities. The obvious origin of this difference is that the longitudinal modes are distributed symmetrically on both sides of the resonant mode, while the transverse resonances ($p=1,2,\ldots$) lie only on one side of the resonant mode.

Another significant difference between the present theory and its plane-wave counterpart is the basic role played by the modal functions in assigning a different spatial structure to the possible field configurations [compare the $A_p(\rho,\eta)$ modes with the functions $\exp(ik_nL\eta)$]. One of the immediate consequences of this fact is that all the field fluctuation variables are coupled to one another to form an infinite system of linear equations [Eqs. (4.9)]. In contrast, the corresponding fluctuation equations for the plane-wave theory[6(g)] break up into an infinite set of (2×2) blocks.

An important and fundamental difference between our model and earlier plane-wave analyses is that our calculations predict the existence of unstable behaviors in the rate-equation regime ($\partial P/\partial t=0$) and even in the limit when both atomic variables are eliminated adiabatically ($\partial P/\partial t=\partial D/\partial t=0$). This result stands in striking contrast with the well-known behavior of the plane-wave Maxwell-Bloch equations, which are always stable in the rate equation and in the full adiabatic elimination regime.

It is interesting to compare the setting and the results of this paper with a recent analysis by Lugiato and Lefever[34] dealing with the spontaneous formation of space instabilities. An important difference is that the low threshold temporal pulsations described in this paper require a radial intermode spacing $\delta\omega_1$ of the order of the longitudinal mode spacing [i.e., $\delta\omega_1'=O(1)$]. The emergence of spatial instabilities requires, instead, that the transverse modes have overlapping profiles in frequency and this implies that $\delta\omega_1'=O(\kappa')$.

In a sense this paper is complementary to the one cited in Ref. 34; of course, the medium is active in our case and not driven by an injected signal, in contrast to the situation described in Ref. 34; furthermore, the cavity geometry is of the ring type with two spherical mirrors, while the resonator of Ref. 34 is a Fabry-Perot. Both studies, however, deal with the competition between longitudinal and transverse modes. In our case the instability is accompanied by temporal oscillations with a frequency of the order of the radial intermode spacing; in the case of Ref. 34 the coexisting transverse and longitudinal modes are synchronous with one another and produce stationary spatial patterns.

ACKNOWLEDGMENTS

This work was partially supported by a contract with the U.S. Army Research Office (Durham, N.C.), a NATO travel grant, the European Economic Community (EEC) twinning project on Dynamics of Nonlinear Optical Systems, and by a Joseph H. deFrees grant of the Research Corporation. One of us (L.M.N.) wishes to express gratitude to Dr. Francis K. Davis for his continued support and encouragement.

APPENDIX A: DERIVATION OF THE BOUNDARY CONDITIONS (3.8d)

With reference to Fig. 1, we represent the boundary conditions with the formal statement

$$E(r,-L/2,t)=\mathcal{R}\wp_{1\to 3'}E\left[r,L/2,t-\frac{\Lambda-L}{c}\right], \tag{A1}$$

where E is the cavity field, the coordinates $z=-L/2$ and $z=L/2$ correspond to positions 3′ and 1, respectively, $\wp_{1\to 3'}$ is a propagation operator between the indicated points, and $\mathcal{R}$ is a reflection operator that accounts both for the reduction in the field amplitude and possible curvature effects upon reflection.

Next we introduce the slowly varying field amplitude as in Eq. (3.3) and, with the help of Eq. (A1), we obtain

$$F(r,-L/2,t)=e^{i\omega_0\Lambda/c}\mathcal{R}\wp_{1\to 3'}F\left[r,L/2,t-\frac{\Lambda-L}{c}\right]. \tag{A2}$$

Because we are interested in deriving boundary conditions for the modal amplitudes $f_p(z,t)$, we let

$$F(r,z,t)=e^{-i\delta\omega t}\sum_p A_p(r,z)f_p(z,t), \tag{A3}$$

and from Eq. (A2) we obtain

$$\sum_p A_p(r,-L/2)f_p(-L/2,t)=\exp(i\omega_0\Lambda/c)\exp\left[i\delta\Omega\frac{\Lambda-L}{c}\right]\mathcal{R}\wp_{1\to 3'}\sum_p A_p(r,L/2)f_p\left[L/2,t-\frac{\Lambda-L}{c}\right]. \quad \text{(A4)}$$

The action of the reflection operator is to scale each modal amplitude f_p by an amount $\sqrt{R}$, where R is the power reflection coefficient, and to apply a phase curvature to the modal functions A_p. If we assume, for simplicity, that the phase mirrors are ideal reflectors and that the curved mirrors have the same reflection coefficient, Eq. (A4) can be written in the form

$$\sum_p A_p(3')f_p(-L/2,t)=\exp(i\omega_0\Lambda/c)\exp\left[i\delta\Omega\frac{\Lambda-L}{c}\right]R\times\sum_p f_p\left[L/2,t-\frac{\Lambda-L}{c}\right]\times\mathcal{R}\wp_{1\to 3'}A_p(1), \quad \text{(A5)}$$

where $A_p(1)$ and $A_p(3')$ denote the modal functions at the indicated points. On the other hand, from the properties of the modal functions (see Sec. II) we have

$$\mathcal{R}\wp_{1\to 3'}A_p(1)=A_p(3')e^{-i\omega_p\Lambda/c}, \quad \text{(A6)}$$

where ω_p is defined by Eq. (2.27), so that Eq. (A5) can also be expressed in the form

$$\sum_p A_p(3')f_p(-L/2,t)=\exp(i\omega_0\Lambda/c)\exp\left[i\delta\Omega\frac{\Lambda-L}{c}\right]\times R\sum_p f_p\left[L/2,t-\frac{\Lambda-L}{c}\right]\times A_p(3')e^{-i\omega_p\Lambda/c}. \quad \text{(A7)}$$

This leads to the required result

$$f_p(-L/2,t)=Rf_p\left[L/2,t-\frac{\Lambda-L}{c}\right]e^{-i\delta_p}\times\exp\left[i\delta\Omega\frac{\Lambda-L}{c}\right], \quad \text{(A8)}$$

where we have used the definition $\delta_p=(\omega_p-\omega_0)\Lambda/c$.

APPENDIX B: DERIVATION OF EQS. (3.18)

The starting point is provided again by Eqs. (3.10) and (3.11) for the modal amplitudes f_p and by Eq. (3.8d) for their boundary conditions. It is convenient to introduce a new set of stationary amplitude functions g_p such that

$$f_p(\eta)=g_p(\eta)\exp\left[i\frac{\delta\Omega'}{v}\eta\right]. \quad \text{(B1)}$$

Their space-dependent equation is

$$\frac{\partial g_p}{\partial\eta}=\alpha L(1-i\Delta')\int_0^\infty d\rho\,\rho A_p^*(\rho,\eta)\chi(\rho,\eta)\times\frac{\sum_{p'}A_{p'}g_{p'}}{1+\Delta'^2+\left|\sum_{p'}A_{p'}g_{p'}\right|^2} \quad \text{(B2)}$$

and the boundary conditions are

$$g_p(-1/2)=Rg_p(1/2)\exp[i(\delta\Omega'\gamma_\perp\Lambda/c-\delta_p)]. \quad \text{(B3)}$$

Now we assume that the quantity

$$\varphi_p=\delta\Omega'\gamma_\perp\frac{\Lambda}{c}-\delta_p,\quad p=0,1,2,\ldots \quad \text{(B4)}$$

is of the order of T for some integer value $p=\bar{p}$. In this case the boundary conditions (B3) can be cast into the approximate form

$$g_{\bar{p}}(1/2)-g_{\bar{p}}(-1/2)=T\left[1-i\frac{\varphi_{\bar{p}}}{T}\right]g_{\bar{p}}(1/2)\quad(p=\bar{p}), \quad \text{(B5a)}$$

$$g_p(1/2)-g_p(-1/2)=(1-Re^{i\varphi_p})g_p(1/2)\quad(p\neq\bar{p}). \quad \text{(B5b)}$$

At the same time the spatial integral of Eq. (B2) is

$$g_p(1/2)-g_p(-1/2)=\alpha L(1-i\Delta')\int_{-1/2}^{1/2}d\eta\int_0^\infty d\rho\,\rho A_p^*\chi\frac{\sum_{p'}A_{p'}g_{p'}}{1+\Delta'^2+\left|\sum_{p'}A_{p'}g_{p'}\right|^2}. \quad \text{(B6)}$$

If we combine Eqs. (B5) and (B6) we obtain

$$g_{\bar{p}}(1/2)-g_{\bar{p}}(-1/2)=T\left[1-i\frac{\varphi_{\bar{p}}}{T}\right]g_{\bar{p}}(1/2)=\alpha L(1-i\Delta')\int_{-1/2}^{1/2}d\eta\int_0^\infty d\rho\,\rho A_{\bar{p}}^*\chi\frac{\sum_{p'}A_{p'}g_{p'}}{1+\Delta'^2+\left|\sum_{p'}A_{p'}g_{p'}\right|^2}\quad(p=\bar{p}), \quad \text{(B7a)}$$

$$g_p(1/2)-g_p(-1/2)=(1-Re^{i\varphi_p})g_p(1/2)$$

$$=\alpha L(1-i\Delta')\int_{-1/2}^{1/2}d\eta\int_0^{\infty}d\rho\,\rho A_p^*\chi\frac{\sum_{p'}A_{p'}g_{p'}}{1+\Delta'^2+\left|\sum_{p'}A_{p'}g_{p'}\right|^2}\quad(p\neq\bar{p})\ . \tag{B7b}$$

Equations (B7) lead to the following conclusions:

(i) The difference $g_{\bar{p}}(1/2)-g_{\bar{p}}(-1/2)$ is of the order of T, so that $g_{\bar{p}}$ is uniform along the axial direction.
(ii) The amplitudes g_p with $p\neq\bar{p}$ are of the order of T.

Hence, in the uniform-field limit a possible steady-state solution is characterized by the modal amplitudes $g_{\bar{p}}=O(1)$ and $g_{p\neq\bar{p}}=O(T)$, and the steady state is governed by Eq. (3.18), which generalizes the case of the TEM_{00} steady state described by Eq. (3.17).

---

[1]See, for example, G. Makhov, C. Kikuchi, J. Lambe, and R. W. Terhune, Phys. Rev. **109**, 1399 (1958).

[2]For some early results, see R. J. Collins, D. F. Nelson, A. L. Schawlow, W. Bond, C. G. B. Garrett, and W. Kaiser, Phys. Rev. Lett. **5**, 303 (1960); D. F. Nelson and W. S. Boyle, Appl. Opt. **1**, 181 (1962); T. N. Zubarev and A. K. Sokolov, Dokl. Akad. Nauk SSSR **159**, 539 (1964) [Sov. Phys.—Dokl. **9**, 1006 (1965)].

[3]Some of the early maser studies dealing with unstable behaviors include K. Y. Khaldre and R. V. Khokhlov, Izv. Vyss. Uchebn. Zaved. Radiofiz. **1**, 60 (1958); A. G. Gurtovnick, *ibid.* **1**, 83 (1958); A. N. Oraevskii, Radio Eng. Electron. Phys. (USSR) **4**, 718 (1959).

[4]The first instability studies of homogeneously broadened lasers include A. V. Uspenskii, Radiotekh. Electron. **8**, 1165 (1963) [Radio Eng. Electron. Phys. (USSR) **8**, 1145 (1963)]; **9**, 747 (1964); [**9**, 605 (1964)]; V. V. Korobkin and A. V. Uspenskii, Zh. Eksp. Teor. Phys. **45**, 1003 (1963) [Sov. Phys.—JETP **18**, 693 (1964)]; A. Z. Grazyuk and A. N. Oraevskii, in *Quantum Electronics and Coherent Light,* edited by P.A. Miles (Academic, New York, 1964) Radiotekh. Electron. **9**, 524 (1964) [Radio Eng. Electron. Phys. (USSR) **9**, 424 (1964)]; H. Haken, Z. Phys. **190**, 327 (1966); H. Risken, C. Schmidt, and W. Weidlich, *ibid.* **194**, 337 (1966).

[5]Several reviews have dealt with the subject of laser instabilities. They include A. N. Oraevskii, Kvant. Elekt. Moscow **8**, 130 (1981); N. B. Abraham, Laser Focus **19**, 73 (1983); L. W. Casperson, in *Laser Physics,* Vol. 182 of *Lecture Notes in Physics,* edited by J. D. Harvey and D. F. Walls (Springer-Verlag, Berlin, 1983); J. C. Englund, R. R. Snapp, and W. C. Schieve, in *Progress in Optics,* edited by E. Wolf (North-Holland, Amsterdam, 1984), Vol. XXI, p. 355; N. B. Abraham, L. A. Lugiato, and L. M. Narducci, J. Opt. Soc. Am. B **2**, 7 (1985); J. R. Ackerhalt, P. W. Milonni and M. L. Shih, Phys. Rep. **128**, 205 (1985); R. G. Harrison and D. J. Biswas, Progr. Quantum Electron. **11**, 127 (1986).

[6](a) H. Haken, Phys. Lett. **53A**, 77 (1975); (b) H. Risken and K. Nummedal, J. Appl. Phys. **39**, 4662 (1968); (c) Phys. Lett. **26A**, 275 (1968); (d) R. Graham and H. Haken, Z. Phys. **213**, 420 (1968); (e) L. A. Lugiato, L. M. Narducci, E. V. Eschenazi, D. K. Bandy, and N. B. Abraham, Phys. Rev. A **32**, 1563 (1985); (f) L. M. Narducci, H. Sadiky, L. A. Lugiato, and N. B. Abraham, Opt. Commun. **55**, 370 (1985); (g) L. M. Narducci, J. R. Tredicce, L. A. Lugiato, N. B. Abraham, and D. K. Bandy, Phys. Rev. A **33**, 1842 (1986).

[7]E. Lorentz, J. Atmos. Sci. **20**, 130 (1963).

[8]For an extensive discussion of the Lorenz chaos, see C. T. Sparrow, *The Lorenz Equations: Bifurcations, Chaos, and Strange Attractors* (Springer-Verlag, Berlin, 1982).

[9]J. R. Tredicce, L. M. Narducci, D. K. Bandy, L. A. Lugiato, and N. B. Abraham, Opt. Commun. **56**, 435 (1986).

[10](a) L. A. Lugiato and L. M. Narducci, Phys. Rev. A **32**, 1576 (1985); (b) L. A. Lugiato, M. L. Asquini, and L. M. Narducci, in *Optical Chaos,* edited by J. Chrostowski and N. B. Abraham (SPIE, Bellingham, 1986), SPIE Vol. 667, p. 132.

[11]L. W. Casperson, J. Opt. Soc. Am. B **2**, 62 (1985); **2**, 73 (1985).

[12]D. K. Bandy, L. M. Narducci, L. A. Lugiato, and N. B. Abraham, J. Opt. Soc. Am. B **2**, 56 (1985).

[13]R. Bonifacio and L. A. Lugiato, Opt. Commun. **19**, 172 (1976); Lett. Nuovo Cimento **21**, 517 (1978); see also L. A. Lugiato, in *Progress in Optics,* edited by E. Wolf (North-Holland, Amsterdam, 1984), Vol. XXI, p. 69.

[14]D. E. Grant and H. J. Kimble, Opt. Lett. **7**, 353 (1982); Opt. Commun. **44**, 415 (1983).

[15]L. A. Lugiato, L. M. Narducci, D. K. Bandy, and C. A. Pennise, Opt. Commun. **43**, 281 (1982).

[16]A. T. Rosenberger, L. A. Orozco, and H. J. Kimble, Phys. Rev. A **28**, 2569 (1983); L. A. Orozco, A. T. Rosenberger, and H. J. Kimble, Phys. Rev. Lett. **53**, 2547 (1984); L. A. Orozco, M. G. Raizen, A. T. Rosenberger and H. J. Kimble, in *Optical Bistability III,* edited by H. M. Gibbs, P. Mandel, N. Peyghambarian, and S. D. Smith (Springer-Verlag, Berlin, 1986), p. 327.

[17](a) R. J. Ballagh, J. Cooper, M. W. Hamilton, W. J. Sandle, and D. M. Warrington, Opt. Commun. **37**, 143 (1981); (b) P. D. Drummond, IEEE J. Quantum Electron. **QE-17**, 301 (1981); (c) W. J. Firth and E. M. Wright, Opt. Commun. **40**, 223 (1982); (d) J. V. Moloney and H. M. Gibbs, Phys. Rev. Lett. **48**, 1607 (1982); (e) L. A. Lugiato and M. Milani, Z. Phys. B **50**, 171 (1983); (f) V. J. Bespalov and V. I. Talanov, Pis'ma Zh. Eksp. Teor. Fiz. **14**, 564 (1971) [JETP Lett. **14**, 390 (1971)]; (g) V. I. Bespalov and V. J. Talanov, Zh. Eksp. Teor. Fiz. **60**, 136 (1971) [Sov. Phys.—JETP **33**, 77 (1971)]; (h) K. Konno and H. Suzuki, Phys. Scr. **20**, 382 (1979).

[18]D. W. Mc Laughlin, J. V. Moloney, and A. C. Newell, Phys. Rev. Lett. **54**, 681 (1985).

[19]M. LeBerre, E. Ressayre, A. Tallet, K. Tai, H. M. Gibbs, M. C. Rushford, and N. Peyghambarian, J. Opt. Soc. Am. B **1**, 591 (1984); J. F. Valley, H. M. Gibbs, M. W. Derstine, R. Pon, K. Tai, M. LeBerre, E. Ressayre, and A. Tallet, in *Opti-*

cal Bistability III, edited by H. M. Gibbs, P. Mandel, N. Peyghambarian, and S. D. Smith (Springer-Verlag, Berlin, 1986), p. 327; M. W. Derstine, H. M. Gibbs, F. A. Hopf, J. F. Valley, *ibid.*, p. 342.

[20]J. V. Moloney, M. R. Belic, and H. M. Gibbs, Opt. Commun. **41**, 379 (1982); J. V. Moloney, Phys. Rev. Lett. **53**, 556 (1984).

[21]L. W. Casperson, IEEE J. Quantum Electron. **QE-10**, 629 (1974); J. Opt. Soc. Am. **66**, 1373 (1976); L. W. Casperson and S. D. Lunnam, Appl. Opt. **14**, 1193 (1975).

[22]G. Stephan and H. Taleb, J. Phys. (Paris) **42**, 1623 (1981); G. Stephan and M. Trumper, Phys. Rev. A **28**, 2344 (1983).

[23]V. S. Idiatulin and A. V. Uspenskii, Opt. Acta **21**, 773 (1974).

[24]L. A. Lugiato and M. Milani, Opt. Commun. **46**, 57 (1983).

[25]L. A. Lugiato, R. J. Horowicz, G. Strini, and L. M. Narducci, Phys. Rev. A **30**, 1366 (1984).

[26]R. Bonifacio and L. A. Lugiato, Lett. Nuovo Cimento **21**, 505 (1978).

[27]L. A. Lugiato, L. M. Narducci, and M. F. Squicciarini, Phys. Rev. A **34**, 3101 (1986).

[28]As already mentioned, these results are not in accord with the experimental findings; the issue here is that the uniform-field limit of the plane-wave model and its exact counterpart are in satisfactory agreement with one another over a wider range of parameter space than might be expected at first sight.

[29]L. A. Lugiato, F. Prati, L. M. Narducci, P. Ru, J. R. Tredicce, and D. K. Bandy, Opt. Commun. **64**, 344 (1987).

[30]P. Ru, L. M. Narducci, J. R. Tredicce, D. K. Bandy, and L. A. Lugiato, Opt. Commun. **63**, 310 (1987) [this paper makes extensive use of the classic results by H. Kogelnik and T. Li, Appl. Opt. **5**, 1150 (1966) and by H. Kogelnik, in *Lasers: A Series of Advances,* edited by A. K. Levine (Marcel-Dekker, New York, 1966), Vol. I, p. 295]; see also A. Yariv, *Optical Electronics,* 3rd ed. (Holt, Rinehart, and Winston, New York, 1985); A. E. Siegman, *Lasers* (University Science Books, Mill Valley, 1986).

[31]W. J. Witteman and G. J. Ernst, IEEE J. Quantum Electron. **QE-11**, 198 (1975).

[32]L. A. Lugiato and M. Milani, J. Opt. Soc. Am. B **2**, 15 (1985).

[33]In a nutshell, the linearized eigenvalues of the plane-wave theory, for each value of the longitudinal index n, are solutions of a quadratic equation: one of the roots of this equation can be associated with the amplitude and the other with the phase variable. Here the linearized eigenvalues are given by first-degree equations [Eq. (4.23b)] and a natural distinction between the two classes of phenomena is no longer possible on this basis.

[34]L. A. Lugiato and R. Lefever, Phys. Rev. Lett. **58**, 2209 (1987).